

Molecular systematics of the Hyaenidae: Relationships of a relictual lineage resolved by a molecular supermatrix

Klaus-Peter Koepfli^{a,*}, Susan M. Jenks^b, Eduardo Eizirik^c, Tannaz Zahirpour^a,
Blair Van Valkenburgh^a, Robert K. Wayne^a

^a Department of Ecology and Evolutionary Biology, University of California, Los Angeles, CA 90095-1606, USA

^b Departments of Biology and Psychology, The Sage Colleges, Troy, NY 12180, USA

^c Faculdade de Biociências, PUCRS, Av. Ipiranga, 6681, Prédio 12, Porto Alegre, RS 90619-900, Brazil

Received 12 June 2005; accepted 31 October 2005

Abstract

The four extant species of hyenas (Hyaenidae; Carnivora) form a morphologically and ecologically heterogeneous group of feliform carnivorans that are remnants of a formerly diverse group of mammalian predators. They include the aardwolf (*Proteles cristatus*), a termite-feeding specialist, and three species with a craniodental morphology adapted to cracking the bones of prey and/or carcasses, the spotted hyena (*Crocuta crocuta*), brown hyena (*Parahyaena brunnea*), and striped hyena (*Hyaena hyaena*). Hyenas have been the subject of a number of systematic studies during the last two centuries, due in large part to the extensive fossil record of the group, with nearly 70 described fossil species. Morphological studies incorporating both fossil and living taxa have yielded different conclusions regarding the evolutionary relationships among living hyenas. We used a molecular supermatrix comprised of seven nuclear gene segments and the complete mitochondrial cytochrome *b* gene to evaluate phylogenetic relationships among the four extant hyaenid species. We also obtained sequence data from representative species of all the main families of the Feliformia (Felidae, Herpestidae, and Viverridae) to estimate the sister group of the Hyaenidae. Maximum parsimony and maximum likelihood analyses of the supermatrix recovered identical topologies. Furthermore, Bayesian phylogenetic analyses of the supermatrix, with among-site rate variation among data partitions parameterized in three different ways, also yielded the same topology. For each phylogeny reconstruction method, all but two nodes received 100% bootstrap or 1.00 posterior probability nodal support. Within the monophyletic Hyaenidae, *Parahyaena* and *Hyaena* were joined together, with *Crocuta* as the sister to this clade, and *Proteles* forming the most basal lineage. A clade containing two species of mongoose (core Herpestidae) plus *Cryptoprocta ferox* (currently classified in Viverridae) was resolved as the sister group of Hyaenidae. The pattern of relationships among the three bone-cracking hyaenids (*Crocuta*, *Hyaena*, and *Parahyaena*) is incongruent with recent cladistic assessments based on morphology and suggests the need to reevaluate some of the morphological characters that have been traditionally used to evaluate relationships among hyenas. Divergence time estimates based on a Bayesian relaxed molecular clock indicates that hyaenids diverged from their feliform sister group 29.2 MYA, in the Middle Oligocene. Molecular clock estimates also suggest that the origin of the aardwolf is much more recent (10.6 MYA) than that implied by a cladistic analysis of morphology (~20 MYA) and suggests that the aardwolf is possibly derived from a bone and meat eating lineage of hyaenids that were present in the Late Miocene. [Hyaenidae; phylogeny; cytochrome *b*; nuclear gene segments; *Proteles*; *Crocuta*; *Hyaena*; *Parahyaena*.]

© 2005 Elsevier Inc. All rights reserved.

Keywords: Hyaenidae; Phylogeny; Cytochrome *b*; Nuclear gene segments; *Proteles*; *Crocuta*; *Hyaena*; *Parahyaena*

* Corresponding author. Fax: +1 310 206 3987.

E-mail address: klausk@lifesci.ucla.edu (K.-P. Koepfli).

“There are few animals, whose history has passed under the consideration of naturalists, that have given occasion to so much confusion and equivocation as the Hyena has done. It began very early among the ancients, and

the moderns have fully contributed their share.” (Bruce, 1790 cited in Kruuk, 1972)

1. Introduction

The Hyaenidae is one of the smallest families of the Carnivora, with a mere four extant species placed in four genera: *Crocuta* (spotted hyena), *Hyaena* (striped hyena), *Parahyaena* (brown hyena) and *Proteles* (aardwolf); (Wozencraft, 1993). This meager extant diversity contrasts sharply with the nearly 70 fossil species that have been described for the family (Werdelin and Solounias, 1991). Biochemical and paleontological data suggest that hyaenids first arose from stem feliforms in the Late Oligocene, about 25 million years ago (MYA); (Werdelin and Solounias, 1991). Hyaenids reached their peak diversity in the Late Miocene, with 20–30 species present during this time, after which they precipitously declined, eventually leaving four surviving species (Werdelin and Solounias, 1991). The four extant species can therefore be considered taxonomic relicts, the remnants of a once diverse group (Brown and Lomolino, 1998; Simpson, 1953).

Extant hyenas form a morphologically and ecologically heterogeneous group of carnivorans. *Proteles cristatus*, the aardwolf, is a diminutive hyaenid (8–14 kg) with greatly reduced premolars and molars and very broad hard palate and large tongue (Koehler and Richardson, 1990). These features are associated with the aardwolf's termite diet, which it collects by licking from the soil surface, making the aardwolf one of only two myrmecophagous species in the extant Carnivora (the other being the sloth bear, *Melursus ursinus*). Aardwolves are socially monogamous, but primarily solitary foragers except when accompanied by cubs (Richardson and Coetzee, 1988). At the other extreme is the spotted hyena, *Crocuta crocuta*, a large (40–86 kg) cursorial hypercarnivore that uses robust premolars to crush bones, which are then ingested. Spotted hyenas live in large matrilineal social groups known as clans whose members hunt cooperatively (Kruuk, 1972; Mills, 1990). Female spotted hyenas are highly aggressive, tend to be larger than males, and have male-like genitalia with a pseudophallus and pseudoscrotum. The brown hyena (*Parahyaena brunnea*) and the striped hyena (*Hyaena hyaena*) are also large in size (28–48 kg and 25–55 kg, respectively) and have dentitions with robust premolars for crushing bones (Mills, 1982, 1990, 1999; Rieger, 1981). These two species are primarily scavengers, although they will also hunt prey smaller or larger than themselves (Mills, 1990; Rieger, 1981). Brown and striped hyenas may form small clans, but both species forage solitarily (Drea et al., 1999; Mills, 1990). Carnassials of *Crocuta*, *Hyaena*, and *Parahyaena* are elongate and well adapted for slicing meat. The similarities among these three species (referred to hereafter as bone-cracking hyaenids) as well as their first occurrence in the fossil record suggests that they evolved relatively recently from a common ancestor, whereas the divergent morphology of the aardwolf suggests it evolved from a more distant ancestor early in hyaenid evolution (Werdelin and Solounias, 1991).

The abundant fossil material available for hyaenids has stimulated a number of paleontologists during the last two centuries to examine evolutionary relationships among taxa within the family, including relationships between fossil taxa and the four living species. Prior to the emergence of cladistics, taxa were grouped together according to overall morphological similarity. With regard to *Crocuta*, *Hyaena*, and *Parahyaena*, two different phylogenetic hypotheses were proposed by paleontologists. The first explicit discussion of hyaenid phylogeny, presented in the form of a key, was that of Gaudry (1862–1867). He considered *H. hyaena* and *P. brunnea* to be more closely related to one another than either is to *C. crocuta*, a hypothesis that was later supported by Pilgrim (1932), Ewer (1955), Theinius (1966), and Hendey (1974). However, it should be noted that Hendey (1974) regarded *H. hyaena* and *P. brunnea* as only distantly related to one another, having diverged in the Miocene, and that *P. brunnea* shared a more recent common ancestry with species of the extinct genus *Pachycrocuta*. As a consequence of this, he named a new subgenus, *Parahyaena*, for *P. brunnea*. Prior to Hendey (1974), *P. brunnea* had been classified as *Hyaena brunnea*, as most authors considered the brown and striped hyenas to be closely related based on morphological similarity. *Parahyaena* was eventually elevated to full generic rank by Werdelin and Solounias (1991). The second hypothesis, proposed by Schlosser (1890), suggested that *P. brunnea* and *C. crocuta* were more closely related than either is to *H. hyaena*. This second hypothesis was supported in the first cladistic analysis of hyaenid phylogeny (Galiano and Frailey, 1977). Due to its highly reduced dentition and other unique features associated with its specialized diet of termites, the aardwolf was seen as a very distant relative of the other hyenas and was often placed in a subfamily or family of its own, the Protelinae or Protelidae.

More recently, Werdelin and Solounias (1991) have addressed the issue of hyaenid interrelationships from a paleontological and morphological perspective. One of the most significant results of this work is that, despite a thorough survey of the skull, dentition and selected areas of the postcranial skeleton, very few phylogenetically informative characters were found. This is largely due to the majority of characters with more than one character state being uniquely derived in *C. crocuta*. Werdelin and Solounias (1991) conducted two different analyses in examining the relationships among living taxa. In the first, *Proteles cristatus* was excluded from the phylogenetic analysis (because most dental characters are absent in this species due to its reduced dentition) and an attempt was made to polarize characters on an a priori basis using outgroup and ontogenetic information. The most parsimonious tree united *P. brunnea* and *C. crocuta* as sister taxa. When *P. cristatus* was included in the second analysis, trees with either *P. brunnea* or *H. hyaena* as sister taxon to *C. crocuta* were equally parsimonious. Werdelin and Solounias (1991) found that a tree one step longer than the two equally parsimonious trees was the traditional one that grouped

P. brunnea and *H. hyaena* as sister taxa. Based on these analyses, the authors concluded that “...the Recent Hyaenidae offer no firm data in support of a resolved scheme of interrelationships” (Werdelin and Solounias, 1991, p. 62).

Despite difficulties with inferring interrelationships among living taxa by themselves, Werdelin and Solounias (1991) conducted additional phylogenetic analyses that included the four living taxa plus 57 “reasonably well known” fossil taxa. The phylogenetic hypothesis they generated places *Proteles* near the base of the hyaenid tree, allying this genus with the extinct genus *Plioviverrops*, a small, mongoose-like insectivore/omnivore whose fossil record extends from the Early to Late Miocene, 16–5 MYA (Werdelin and Solounias, 1991, 1996). This hypothesis implies that *Proteles* has an early origin (~20 MYA) and that it is distantly related to the other living taxa. However, the fossil record of *Proteles* only extends to the Early Pleistocene (1.5 MYA) and suggests a more recent origin for this genus. Resolving the discrepancy between the cladistic age and the fossil age of *Proteles* is important for understanding the ecological context that led to the evolution of morphological specializations associated with the myrmecophagous diet of the aardwolf. As for *Parahyaena*, *Hyaena*, and *Crocota*, these taxa are part of the most derived clade within the Hyaenidae (and hence, among the most recently evolved), representing taxa with advanced bone-cracking adaptations (such as greatly enlarged premolars). Interestingly, in this phylogenetic scheme, *Hyaena* is placed as more closely related to *Crocota* than it is to *Parahyaena*. This working phylogenetic hypothesis has been used in many subsequent studies of hyaenid morphological and ecological evolution (e.g., Werdelin, 1996a,b; Werdelin and Solounias, 1996) and therefore forms the modern view of hyaenid interrelationships based on morphology.

The phylogeny of extant hyaenids has been examined using karyotypic and mitochondrial DNA data. Wurster and Benirschke (1968) found that *Proteles*, *Hyaena* and *Crocota* were nearly identical in karyotype, suggesting a close relationship among these three genera. Jenks and Werdelin (1998) used complete sequences of the mitochondrial cytochrome *b* gene from the four living hyaenids plus two distant outgroups (cat, *Felis catus*, and harbor seal, *Phoca vitulina*) and found that *Hyaena* and *Parahyaena* were sister taxa, but also that *Crocota* and *Proteles* were united as sisters with 100% bootstrap support. This latter relationship had never before been suggested in prior studies and the authors suspected that long branch attraction (Felsenstein, 1978) had drawn *Proteles* and *Crocota* together. Consequently, they conducted phylogenetic analyses using transversion parsimony or third position transversions only. The resulting phylogenetic trees placed *Proteles* as the most basal hyaenid, with *Crocota* forming the sister group to *Hyaena* plus *Parahyaena* (Jenks and Werdelin, 1998). Taken altogether, previous morphological and molecular phylogenetic analyses have supported every possible combination of relationships between extant bone-cracking hyaenids.

Higher-order phylogenetic relationships between hyaenids and other feliform families have also proven controversial.

Based on analyses of morphologic data, two phylogenetic hypotheses have been supported. First, a sister relationship of hyenas and cats (Felidae) has been suggested (Wozencraft, 1993; Wyss and Flynn, 1993). This hypothesis is also supported in a supertree analysis of the Carnivora (Bininda-Emonds et al., 1999). Second, a sister relationship between hyenas and mongooses (Herpestidae) has also been proposed (Hunt, 1987, 1989; Veron, 1995). DNA–DNA hybridization data have provided weak support for a relationship between hyenas and civets (Viverridae); (Wayne et al., 1989). Most recently, studies using mitochondrial and/or nuclear gene sequences, but using only *Crocota* as the sole representative of Hyaenidae, have demonstrated a sister-group relationship between herpestids and hyaenids (Flynn and Nedbal, 1998; Flynn and Nedbal, 1998; Gaubert and Veron, 2003; Yoder et al., 2003; Yu et al., 2004). Therefore, in addition to controversial aspects regarding the relationships among hyaenid species, the specific position of the family within the suborder Feliformia remains uncertain.

Here, we use a molecular supermatrix comprised of seven nuclear gene segments and the mitochondrial cytochrome *b* gene, from all four living hyaenids and eight taxa representing species from the other three feliform families, to reconstruct phylogenetic relationships among these taxa. The aims of our study are to: (1) estimate the relationships among extant hyaenids; (2) assess the divergence time of *Proteles* from the other three hyaenids to distinguish whether the aardwolf evolved early or late in hyaenid evolution; and (3) determine the sister group (Felidae, Herpestidae, or Viverridae) of the Hyaenidae. We also conducted phylogenetic analyses in which we combined our molecular supermatrix with a modified version of the morphological character matrix from Werdelin and Solounias (1991) to evaluate the degree of congruence and incongruence between molecular and morphological data sets.

2. Materials and methods

2.1. Taxon sampling

Tissue samples were obtained from two individuals of each hyena species except *H. hyaena* (Table 1). Samples from two or three representative species each of the Felidae, Herpestidae, and Viverridae were included to determine the sister group of the Hyaenidae (Table 1). Our taxon sampling includes *Cryptoprocta ferox* and *Nandinia binotata*, which most classifications of the Carnivora assign to the Viverridae (e.g., Wozencraft, 1993). Recent molecular studies, however, indicate that *Cryptoprocta* is part of an endemic radiation on Madagascar that is sister to the core Herpestidae (Yoder et al., 2003) and that *Nandinia* is the most basal extant feliform taxon (Flynn and Nedbal, 1998). These and other studies (e.g., Gaubert and Veron, 2003) suggest that the taxonomy of the Viverridae is in need of substantial revision. Two species from the Canidae (Caniformia) were used as distant outgroups to root feliform taxa (Table 1).

Table 1
Species, common names and source information for taxa used in this study

Taxon	Common name	Source
<i>Feliformia</i>		
Hyaenidae		
<i>Crocuta crocuta</i> (2)	Spotted hyena	Field Station for Behavior Research Hyena Project, University of California, Berkeley
<i>Hyaena hyaena</i>	Striped hyena	Center for Reproduction on Endangered Species, Zoological Society of San Diego
<i>Parahyaena brunnea</i> (2)	Brown hyena	Center for Reproduction on Endangered Species, Zoological Society of San Diego
<i>Proteles cristatus</i> (2)	Aardwolf	Center for Reproduction on Endangered Species, Zoological Society of San Diego
Felidae		
<i>Lynx canadensis</i>	Canadian lynx	Kenai National Wildlife Refuge, Alaska
<i>Panthera leo</i>	Lion	Johannesburg Zoo, South Africa
Viverridae		
<i>Cryptoprocta ferox</i>	Fossa	Center for Reproduction on Endangered Species, Zoological Society of San Diego
<i>Genetta tigrina</i>	Large-spotted genet	Kenya; collected by R.K. Wayne, University of California, Los Angeles
<i>Nandinia binotata</i>	African palm civet	Cameroon; collected by D.B. Pires, University of California, Los Angeles
<i>Paradoxurus hermaphroditus</i>	Common palm civet	Museum of Vertebrate Zoology 186574, University of California, Berkeley
Herpestidae		
<i>Herpestes javanicus</i>	Javan mongoose	Museum of Vertebrate Zoology 186570, University of California, Berkeley
<i>Mungos mungo</i>	Banded mongoose	Kenya; collected by R.K. Wayne, University of California, Los Angeles
<i>Caniformia</i>		
Canidae		
<i>Canis lupus</i>	Wolf	Inuvik, Northwest Territories, Canada; collected by Peter Clarkson
<i>Vulpes vulpes</i>	Red fox	United Kingdom; collected by Eli Geffen, University of Tel Aviv

Numbers in parentheses indicate number of individuals sequenced if >1. Classification according to [Wozencraft, 1993](#).

2.2. Laboratory methods

We extracted total genomic DNA from tissue samples using phenol/chloroform methods followed by precipitation with ethanol or with a QIAamp DNA Mini Kit (Qiagen, Valencia, CA) according to the manufacturer's protocol. We amplified exon or exon/intron segments from the following seven nuclear genes using the primers shown in [Table 2](#): APOB, CHRNA1, COL10A1, GHR, GNAT1, RAG1, and WT1. For several of these loci, we designed internal primers for use in both amplification and sequencing. We also obtained sequences of the complete mitochondrial cytochrome *b* (cyt *b*) gene using a combination of published primers ([Table 2](#)). All gene segments were amplified by the polymerase chain reaction (PCR) in an MWG-Biotech Primus 96 Plus thermal cycler with the following conditions: 28–30 cycles of 94°C for 30 s, 52–54°C for 30 s, 72°C for 45 s, and one cycle of 72°C for 5 min. Each 50 µl reaction contained 35.7 µl sterile double-distilled water, 5 µl 10× PCR buffer, 5 µl of 25 mM MgCl₂, 1 µl of 10 mM dNTP mix, 1 µl of both 25 pM/µl forward and reverse primers, 0.3 µl *Taq* polymerase (Sigma–Aldrich, St. Louis, MO), and 1 µl of 0.1–1 µg genomic DNA. All PCRs included a negative control (no DNA). Amplification products were size-fractionated through 1% agarose/Tris–acetic acid–EDTA gels and the appropriate band was excised and then purified with an Ultra Clean Kit (MoBio Laboratories, Solana Beach, CA). Products were sequenced using the amplification primers and the CEQ Dye Terminator Cycle Sequencing Quick Start Kit (Beckman–Coulter, Fullerton, CA). Sequencing reactions were precipitated according to the manufacturer's protocol and run on a CEQ2000XL automated capillary sequencer (Beckman–

Coulter, Fullerton, CA). Chromatographs were checked for accuracy and edited using Sequencher 3.1 (Gene Codes, Ann Arbor, MI). Despite repeated efforts at modifying thermal cycling and/or sequencing conditions, we were unable to obtain GNAT1 sequences from *Nandinia binotata* and *Paradoxurus hermaphroditus* or RAG1 sequences from *Canis lupus* and *Vulpes vulpes*. These taxa were coded with question marks (missing data) for the two loci in the combined phylogenetic analyses. APOB sequences from *Crocuta crocuta*, *Panthera leo*, *Nandinia binotata*, and *Vulpes vulpes* were from the study by [Amrine-Madsen et al. \(2003\)](#).

2.3. Sequence alignment and treatment of gaps

Sequences for all loci were aligned by eye. Several nuclear gene segments contained insertions and/or deletions (indels) that necessitated introduction of gaps into sequences. Alignment of sequences where indels occurred was largely unambiguous. However, both GHR and WT1 had regions that contained microsatellite sequences that varied in length among taxa making unambiguous alignment of these regions difficult. Further, WT1 contained a small region that was difficult to align unambiguously. Therefore, we excluded nine base pairs (bp) from the GHR alignment and 107 bp from the WT1 alignment (a total of 116 bp) for all phylogenetic analyses. For maximum parsimony analyses, potential phylogenetic signal contained in indels was recovered by coding gaps according to the method of [Barriel \(1994\)](#). This method treats indels as single events regardless of length or complexity and uses question marks associated with subsequent substitutions that are contained within the indels, thereby minimizing tree

Table 2

Gene abbreviation, type of sequence, and forward (F) and reverse (R) primer sequences for nuclear and mitochondrial gene segments amplified and sequenced in this study

Gene	Type of sequence	Primer sequences (5' → 3')	Reference
APOB	Exon	F: GTG CCA GGT TCA ATC AGT ATA AGT R: CCA GCA AAA TTT TCT TTT ACT TCA A	Amrine-Madsen et al., 2003 Jiang et al., 1998
CHRNA1	Exon/intron	F: GAC CAT GAA GTC AGA CCA GGA G R: GGA GTA TGT GGT CCA TCA CCA T	Lyons et al., 1997
COL10A1	Exon	F: ATT CTC TCC AAA GCT TAC CC R: GCC ACT AGG AAT CCT GAG AA F: GAT AAG ATT CTG TAT AAC AGG C R: TAG GAA TCC TGA GAA GGA GG	Venta et al., 1996 internal primer; this study internal primer; this study
GHR	Exon/intron	F: CCA GTT CCA GTT CCA AAG AT R: TGA TTC TTC TGG TCA AGG CA F: CTG TCC TAT GTT GAG AGC ATT TGC R: GAA ACA TTT TCC TCC AGA AGG G	Venta et al., 1996 internal primer; this study internal primer; this study
GNAT1	Exon/intron	F: AGC ACC ATC GTC AAG CAG A R: CTG GAT ACC CGA GTC CTT C	Brouillette et al., 2000
RAG1	Exon	F: GCT TTG ATG GAC ATG GAA GAA GAC AT R: GAG CCA TCC CTC TCA ATA ATT TCA GG	Teeling et al., 2000
WT1	Exon/intron	F: GAG AAA CCA TAC CAG TGT GA R: GTT TTA CCT GTA TGA GTC CT F: GGA AGC ATC CCA CAT TTC TCT TGC R: GAA TCA CAG GCT ACA AAC TGG GAC	Venta et al., 1996 internal primer; this study internal primer; this study
Cyt <i>b</i>	Mitochondrial coding	F: CGA AGC TTG ATA TGA AAA ACC ATC GTT G R: AAA CTG CAG CCC CTC AGA ATG ATA TTT GTC CTC A F: GCA AGC TTC TAC CAT GAG GAC AAA TAT C R: TAG TTG TCA GGG TCT CCT AG R: AAC TGC AGT CAT CTC CGG TTT ACA AGA C	L14724; Irwin et al., 1991 H15149; Kocher et al., 1989 L15162; Irwin et al., 1991 L15408; Irwin et al., 1991 H15494; Koepfli and Wayne, 1998 H15915; Irwin et al., 1991

Gene names are APOB, apolipoprotein B; CHRNA1, cholinergic receptor, nicotinic, α polypeptide 1 precursor; COL10A1, collagen type X α I; GHR, growth hormone receptor; GNAT1, guanine nucleotide binding protein, α transducing polypeptide 1; RAG1, recombination activating protein 1; WT1, Wilms tumor 1; Cyt *b*, cytochrome *b*.

length. Gaps were treated as missing characters in maximum likelihood and Bayesian analyses.

2.4. Phylogeny estimation

2.4.1. Maximum parsimony

We reconstructed most parsimonious trees for the eight individual loci, combined nuclear loci, and a combined supermatrix (nuclear and mitochondrial sequences) using PAUP* (Swofford, 2002). All characters were equally weighted in all analyses. For individual nuclear gene segments and combined analyses of concatenated nuclear data and supermatrix, we performed branch and bound searches, with the initial upper bound computed via stepwise addition, the 'furthest' taxon sequence added to the search trees, and the 'Multrees' option (saving of all optimal trees) in effect. Because branch and bound searches are inefficient for data sets containing high amounts of homoplasy, a heuristic search was employed for the *cyt b* data set, using 100 replicates of stepwise addition and tree bisection–reconnection (TBR) branch swapping. We evaluated branch support with 1000 pseudoreplicates of bootstrapping and the same branch and bound (nuclear gene segments and combined analyses) or heuristic (*cyt b*) search conditions used to reconstruct the most parsimonious tree(s). We used the maximum parsimony bootstrap analyses to detect if there was any significant incongruence among topologies derived from the eight individual

data sets, using the value of $\geq 70\%$ as our criterion for significant bootstrap support (e.g., Flynn and Nedbal, 1998).

2.4.2. Model selection

Modeltest 3.06 (Posada and Crandall, 1998) was used to estimate the model and parameters of DNA evolution that best fit each of the following data partitions: (a) individual loci; (b) combined nuclear DNA data; and (c) combined supermatrix. Best-fit models were chosen among a series of nested models according to the Akaike information criterion (AIC; Akaike, 1974) as implemented in Modeltest.

2.4.3. Maximum likelihood

Maximum likelihood (ML) analyses of the combined supermatrix were performed using PAUP*, with the best-fitting model and associated parameters determined via Modeltest specified in the tree search. We employed heuristic searches with 100 replicates of random stepwise addition and tree bisection–reconnection branch swapping. Three hundred pseudoreplicates of bootstrapping with one replicate of random stepwise addition and the 'Multrees' option turned off (DeBry and Olmstead, 2000) were employed to measure support for the ML tree.

2.4.4. Bayesian analyses

We used MrBayes v2.01 (Huelsenbeck, 2000) and MrBayes 3 (Ronquist and Huelsenbeck, 2003) to perform several

different Bayesian analyses in order to examine sensitivity of the posterior probability and parameter estimates when the supermatrix was analyzed under alternative models of varying complexity. We used the best-fitting model of evolution selected with Modeltest for the likelihood function component of Bayes' rule, as applied to phylogenetic analysis (Huelsenbeck et al., 2001).

Model parameters, along with tree topologies and branch posterior probabilities, were estimated as part of the analyses. The empirical nucleotide frequencies of the supermatrix were specified as priors for all analyses.

We parameterized models in several different ways. Three different Markov Chain Monte Carlo (MCMC) analyses were conducted in which the eight data sets were assumed to all evolve under the same model of evolution (i.e., GTR) but differed in the way the among-site rate variation, as approximated with the gamma distribution shape parameter (α), was partitioned among and within the eight data sets. Model 1 included a parameter for the proportion of invariable sites (I) and applied a single gamma shape parameter for the supermatrix (no partitioning of among-site rate variation). Model 2 partitioned the gamma shape parameter among the eight data sets that comprise the supermatrix by defining the eight partitions and using the "rates = sitespecificgamma" in the MrBayes v2.01 command block. Model 3 partitioned the gamma shape parameter among the seven nuclear gene data sets and among the three codon positions of *cyt b* using the same command for "rates" as in Model 2. Therefore, models 1–3 employed 2, 9, and 11 parameters, respectively, for the among-site rate variation, along with the other parameters of the best-fit model. A single GTR substitution rate matrix was applied across the supermatrix for all three models. MCMC analyses used one cold and three heated chains that ran for 1,000,000 generations, from which trees were sampled every 100 generations. We conducted three independent MCMC runs for each of the three models to confirm that the stationarity of likelihood values and parameter estimates were consistent among runs. Burn-in plots were examined to evaluate the number of generations elapsed before likelihood scores had achieved stationarity. For each run, consensus trees with node posterior probabilities were generated based on 9000 or 7000 trees, depending on the model, after the first 1000 or 3000 trees (or 100,000 or 300,000 generations) were discarded as burn-in. Final consensus trees derived from the three independent runs for each model were based on a total of 27,003 (3×9001) or 21,003 (3×7001) trees, depending on the model used (see Section 3).

2.4.5. DNA and morphology

We also evaluated phylogenetic relationships among extant hyenas by combining our molecular supermatrix with morphological characters from the study by Werdelin and Solounias (1991) in a total evidence analysis framework using parsimony (Kluge, 1998). In their original analyses, Werdelin and Solounias' (1991) data matrix contained 26 coded morphological characters for the four hyena spe-

cies plus a 'hypothetical ancestor' that was used as the outgroup (five taxa total). Werdelin and Solounias conducted phylogenetic analyses with and without *P. cristatus* because some dental characters were absent from this species (and therefore could not be coded) due to its highly reduced dentition relative to the three bone-cracking hyaenids. Their data matrix without *Proteles* contained three characters that were excluded from the matrix that included *Proteles* (see Table 1 and Table 2 in Werdelin and Solounias, 1991). We added these three characters (6: stage of reduction in size of the upper first molar relative to the upper fourth premolar; 8: presence or absence of metaconid on the lower first molar; and 11: relative length of paracone and metacone of the upper fourth premolar) to the original 26 character matrix and simply coded them as missing for *P. cristatus*. Furthermore, we discovered that two taxa had been incorrectly coded for two characters, and we changed their codings to make them consistent with original character definitions given by Werdelin and Solounias (1991). Character 39, size of mastoid crest, was originally coded as 0 = short for *P. brunnea* by Werdelin and Solounias (1991). However, these authors state:

"In *H. hyaena*, as well as the outgroups, the mastoid crest ends at the postero-dorsal end of the external auditory meatus. In *P. brunnea* and *C. crocuta*, on the other hand, the mastoid crest continues beyond this point well towards the ventral end of the external auditory meatus, a condition that is probably derived" (Werdelin and Solounias, 1991, p. 56).

Therefore, we coded *P. brunnea* as 1 = long for character 39, a condition shared with *C. crocuta*. We also changed the coding for character 45, size of metacarpal I in *Proteles cristatus*. This species was coded as 1 = reduced in the original analysis, but Werdelin and Solounias (1991) comment:

"This bone is vestigial in *H. hyaena*, *P. brunnea* and *C. crocuta*. This is a derived state uniting these species relative to *Proteles*, where the [metacarpal] I is much larger" (p. 57).

Therefore, we coded *P. cristatus* as 0 = large for character 45, a condition shared with the outgroup. Finally, we note that the coding definitions for character 24, suture between premaxillary and frontal on snout, were reversed in Werdelin and Solounias (1991). Based on the authors' definition for this character, 0 = present, and 1 = absent, rather than the reverse. Nonetheless, taxa were all coded correctly for this character.

For the total evidence analysis, we used two representative taxa of the feliform family that was found to be the sister group of the Hyaenidae based on the supermatrix analyses that included all the taxa. To make the morphology matrix congruent with the supermatrix, we added another hypothetical ancestor with the same codings as the first hypothetical ancestor from the Werdelin and Solounias (1991) study to the morphology matrix (six taxa in total). This strategy assumes that the outgroup taxa used

for the supermatrix and the morphology matrix are equivalent, even though Werdelin and Solounias (1991) could not confidently determine, based on cladistic analysis of morphological characters, which feliform group was the sister group to the hyaenids. Nonetheless, the primitive state codings for the morphological characters in the hypothetical ancestor are based on a detailed evaluation of primitive fossil hyaenids and other feliform groups by Werdelin and Solounias (1991). Therefore, it is not unrealistic to expect that some of these characters would be found in the true feliform sister group of the hyaenids. Given these considerations, we conducted total evidence parsimony analysis using the exhaustive search option in PAUP*. Branch support for the shortest tree was estimated using 1000 pseudoreplicates of bootstrapping with branch and bound search and the same search conditions as described for the molecular supermatrix parsimony analyses. In addition, we used TreeRot 2.0 (Sorenson, 1998) to quantify the Bremer support for each node (Bremer, 1988) and to conduct partitioned Bremer support analyses (PBS) in order to evaluate the relative contribution of the nine data sets (eight gene partitions and one morphology partition) to the total Bremer support at each node.

2.5. Divergence dates

Divergence dates among the sampled taxa were estimated using the Bayesian relaxed clock method developed by Thorne et al. (1998) and Kishino et al. (2001). This approach allows for heterogeneity of substitution rates among branches of the tree (i.e., departures from a strict molecular clock), while incorporating multiple fossil calibrations to constrain node ages. We used the ML topology obtained with the molecular supermatrix and the program *estbranches* to estimate branch lengths and a rate variance–covariance matrix. The program *divtime5b* was then used to estimate divergence dates among all sampled taxa, with 1,000,000 generations run after 100,000 generations of burn-in, and nine fossil constraints obtained from McKenna and Bell (1997) and Turner (1987): (1) minimum of 4 MYA (i.e., *Hyaena*) and (2) maximum of 16.4 MYA for the base of crown Hyaenidae (i.e., *Proteles* vs others); (3) minimum of 16.4 MYA for *Cryptoprocta* vs. core Herpestidae; (4) minimum of 3.58 MYA for *Herpestes* vs. *Mungos*; (5) minimum of 16.4 MYA for *Genetta* vs. *Paradoxurus*; (6) minimum of 5.3 MYA and (7) maximum of 23 MYA for the base of Felidae; (8) minimum of 28.5 MYA for Felidae vs. others; and (9) maximum of 55 MYA for the base of Feliformia (*Nandinia* vs. others). The mean of the prior distribution for the ingroup root age was set at 50 MYA (consistent with McKenna and Bell, 1997; Springer et al., 2003), and its impact on the posterior distribution of node ages was tested empirically. Eleven independent runs were performed to evaluate convergence of point estimates and credibility intervals for divergence dates, to test for consistency among different fossil constraints, and to assess the effect of modifying the prior for root-to-tip age.

3. Results

3.1. Sequence characteristics and incongruence among the data partitions

The total length of the molecular supermatrix alignment, including gaps, was 6218 characters. Five nuclear gene segments (APOB, CHRNA1, GHR, GNAT1, and WT1) contained a total of 56 indels of various lengths. Forty (40) indels were parsimony-informative for a particular feliform family or for differentiating feliforms from the two canid outgroup species. Interestingly, we discovered two large insertions that occurred in different locations in the GHR gene segment. One insertion was 229 or 230 bp in length and found in the two herpestids, *Herpestes javanicus* and *Mungos mungo*, respectively. The other insertion was 194 bp long and occurred 3' to the first insertion in the two canid outgroup species. To utilize the potential phylogenetic signal contained by the indels, we coded them according to the method proposed by Barriel (1994); (see Section 2). When indels were coded in this way, the length of the supermatrix alignment was 5730 characters. Sequences generated for this study were deposited in GenBank under Accession Nos. AY928668–AY928771 (Appendix A).

Among nuclear gene segments that we sequenced, WT1 contained the greatest number of variable and parsimony-informative sites (after exclusion of ambiguously aligned sequences, see Section 2), with APOB and GHR also containing a large number of parsimony-informative sites (Table 3). The *cyt b* gene, however, contained two to three times more variable and parsimony-informative sites than any of these three nuclear gene segments. Additional sequence characteristics, tree statistics from the parsimony analyses, and the best-fitting models and their associated parameters estimated using Modeltest for each of the data partitions are presented in Table 3.

We detected one instance of significant incongruence for the APOB data partition in the separate parsimony analyses of the eight gene segments, using our criterion of $\geq 70\%$ bootstrap support for strongly conflicting nodes. The most parsimonious tree for APOB places the felid clade as the sister group to a clade comprised of the herpestids (including *Cryptoprocta*) and hyaenids, with a bootstrap support of 79%. This conflicts significantly with the most parsimonious trees for CHRNA1, GNAT1, and WT1, which place the viverrid clade as the sister group to herpestids and hyaenids, with a bootstrap support of 77, 91, and 71%, respectively. This latter relationship is also found in the parsimony analyses of GHR, RAG1, and *cyt b*, albeit with weak nodal support (<70%). The COL10A1 gene tree was also incongruent with the other gene trees in several respects, such as finding that *Genetta* and *Paradoxurus* were not monophyletic and placed basally among the feliforms, and the joining of *Nandinia* as the sister to the herpestid clade (including *Cryptoprocta*). These relationships, however, received <50% bootstrap support. Despite the significant incongruence of a single node found in the APOB gene tree, we do not think that this warrants exclusion

Table 3
Sequence characteristics, descriptive statistics from parsimony analyses, and models and substitution parameters derived from Modeltest for each of the eight gene segment partitions and the two combined data partitions

	APOB	CHRNA1	COL10A1	GHR	GNAT1	RAG1	WT1	Cyt <i>b</i>	Nuclear	Supermatrix
No. of nucleotides	938/937	377/344	320/320	1113/675	463/445	1076/1076	791/686	1140	5078/4590	6218/5730
No. variable	203	155	68	215	89	130	217	503	1077	1580
No. parsimony-informative	135	99	49	115	57	71	140	390	666	1056
No. of trees	1	1	2	1	1	3	1	3	1	1
Tree length	24	202	100	270	101	185	281	1479	1390	2869
Retention index	0.911	0.882	0.779	0.897	0.936	0.688	0.841	0.381	0.852	0.623
Model	TVM + G	K81 + G	TIMef + I	TIM + G	TrN + I	K80 + I + G	K81uf + G	TVM + I + G	GTR + G	GTR + I + G
π_A	0.325	0.280	0.263	0.299	0.192	0.265	0.245	0.296	0.275	0.280
π_C	0.217	0.220	0.262	0.186	0.322	0.241	0.221	0.300	0.231	0.245
π_G	0.176	0.250	0.224	0.193	0.290	0.267	0.270	0.135	0.233	0.212
π_T	0.282	0.250	0.251	0.322	0.196	0.227	0.264	0.269	0.261	0.263
I	—	—	0.6846	—	0.5859	0.6556	—	0.4905	—	0.4461
G	0.7845	1.7452	—	0.6677	—	0.6739	0.6388	0.7782	0.4442	0.6396
TS/TV ratio	—	—	—	—	—	3.7689	—	—	—	—
Γ_{AC}	1.4019	1.0000	1.0000	1.0000	1.0000	—	1.0000	40.7453	1.3155	2.6065
Γ_{AG}	5.4906	3.0690	3.9056	2.4134	7.2681	—	4.1523	671.4096	4.4161	6.0604
Γ_{AT}	0.6074	0.4896	0.4384	0.4436	1.0000	—	0.5375	38.5516	0.5582	0.6652
Γ_{CG}	1.3371	0.4896	0.4384	0.4436	1.0000	—	0.5375	2.7985	0.8769	0.6699
Γ_{CT}	5.4906	3.0690	6.0623	3.4420	8.2561	—	4.1523	671.4096	5.1955	11.1836
Γ_{GT}	1.0000	1.0000	1.0000	1.0000	1.0000	—	1.0000	1.0000	1.0000	1.0000

No. of nucleotides, alignment length with gaps included in the alignment/alignment length with gaps coded according to Barriol (1994). π_A , π_C , π_G , and π_T = empirical base frequencies; I, proportion of invariable sites; G, gamma shape parameter; TS/TV, transition/transversion ratio; Γ_{AC} , Γ_{AG} , Γ_{AT} , Γ_{CG} , Γ_{CT} , and Γ_{GT} = rate of substitution for specified nucleotides.

of the APOB data set from a combined analysis of other data gene segments. Instead, the influence of such conflicting phylogenetic signals is best evaluated in the context of a combined analysis of all data (Rokas et al., 2003).

3.2. Combined nuclear data vs. cytochrome *b* gene analyses

Maximum parsimony and likelihood analyses recovered identical topologies when the seven nuclear gene segments were concatenated (Figs. 1A and B). *Nandinia* was strongly supported as the most basal taxon and sister to the remaining feliform clades. Felids formed the next successive clade, which was sister to a group that included core viverrids (*Genetta* and *Paradoxurus*), hepestids, and hyaenids. Within this group, we found that the two herpestids plus *Cryptoprocta* (currently classified in the Viverridae, Wozencraft, 1993) formed the sister group to the hyaenids with 100% bootstrap support in both MP and ML analyses. Within the hyaenids, *Proteles* was the most basal taxon and *Crocota* was sister to the clade comprised of *Hyaena* and *Parahyaena*. Nine of the eleven resolved nodes received 100% bootstrap support in both MP and ML analyses. The two nodes that had bootstrap values <100% had short internal branch lengths, especially in the ML analysis (Fig. 1B). The node between felids and core viverrids had bootstrap support of 99% (MP) and 68% (ML) while the node between *Proteles* and *Crocota* had bootstrap support of 96% (MP) and 84% (ML); (Figs. 1A and B).

Topologies of the MP and ML trees based on the cyt *b* gene data differed slightly from each other as well as from those based on concatenated nuclear gene segments (Figs. 1C and D). The parsimony tree was largely congruent with the nuclear gene tree, except that *Crocota* was placed as the

sister taxon to *Proteles*, although with low bootstrap support (52%). This same grouping was recovered in the ML tree using the TVM + I + G model, except that the bootstrap support was increased to 80%. The ML tree also differed from the combined nuclear gene analyses and the cyt *b* MP tree by placing *Cryptoprocta* as the sister taxon to a clade containing the herpestids and hyaenids. However, this relationship had low bootstrap support (67%).

We examined whether base composition heterogeneity in the cyt *b* data had somehow caused *Proteles* and *Crocota* to be joined together in the MP and ML analyses of these data. Even though we cannot know the true phylogeny, the combined nuclear data provide strong evidence for the relationships among the hyenas in both MP and ML analyses. Therefore, we assessed the possibility that systematic error, such as nonstationary base composition, had influenced the cyt *b* topologies. Among the eight gene segments sequenced, only the cyt *b* gene data was found to be significantly heterogeneous in base composition for both informative sites and all sites, using the χ^2 test of homogeneity of base frequencies as implemented in PAUP* (Swofford, 2002). The COL10A1 gene segment was the only other data partition that was significantly heterogeneous in base frequency for the informative sites. The significant heterogeneity in base composition for the cyt *b* data may bias phylogenetic reconstruction methods that fail to take nonstationary base composition into account (Lockhart et al., 1994). Consequently, we conducted minimum evolution analyses (Rzhetsky and Nei, 1992) of cyt *b* data with bootstrapping (1000 pseudoreplicates) using the LogDet/paralinear distance to correct for possible nonstationary base composition (Lake, 1994; Lockhart et al., 1994). To account for rate

heterogeneity in the LogDet distance calculations (Swofford et al., 1996), we used likelihood evaluation of the three most parsimonious trees from the *cyt b* data to

estimate the proportion of invariable sites (I) under the GTR model. We estimated I to be 0.5449, 0.5449, and 0.5448 for the three trees and used $I=0.5449$ in minimum evolution analyses. The minimum evolution bootstrap consensus tree using LogDet+I transformed distances showed strong support for most feliform family clades, but the relationships among these clades and the position of *Nanidina* and *Cryptoprocta* received <50% bootstrap support (results not shown). Importantly, the relationships among the four hyenas were identical to those found in nuclear gene trees (Figs. 1A and B), except that the node between *Proteles* and *Crocota* only had a bootstrap support of 54%. These results using LogDet+I distances therefore suggest that non-stationary base composition may have affected the MP and ML analyses of the *cyt b* data because neither of these methods alone corrects for such systematic bias.

In general, the *cyt b* gene trees had fewer nodes that were well supported by bootstrap analyses than gene trees based on the combined nuclear data (compare Figs. 1A and B with Figs. 1C and D). The uncorrected pairwise sequence divergence for the *cyt b* gene within the ingroup ranged from 7.6% (*Hyaena* vs. *Parahyaena*) to 19.5% (*Panthera* vs. *Crocota*). In contrast, for the combined nuclear gene data, the sequence divergence ranged from 0.12% (*Hyaena* vs. *Parahyaena*) to 7.7% (*Paradoxurus* vs. *Nandinia*). Multiple substitutions at the same sites in the *cyt b* gene most likely affected the phylogenetic signal at higher levels of sequence divergence. Indeed, as measured by the retention index, *cyt b* data contained a greater amount of homoplasy relative to the individual or combined nuclear gene segment data (Table 3).

3.3. Supermatrix analyses

Parsimony analysis, maximum likelihood analysis, and Bayesian inference of the molecular supermatrix all resulted in identical topologies (Fig. 2). This topology was identical to the one reconstructed based on the combined nuclear data alone (Figs. 1A and B). The 5730 character supermatrix used for the parsimony analyses had 1056 parsimony-informative sites and a tree length of 2869 steps. The retention index for the supermatrix parsimony tree was lower than that for the concatenated nuclear gene tree (0.623 vs. 0.852) as a result of the addition of the more homoplastic *cyt b* data set. The best-fitting model of substitution for the supermatrix determined using Modeltest was the GTR + I + G model (Table 3).

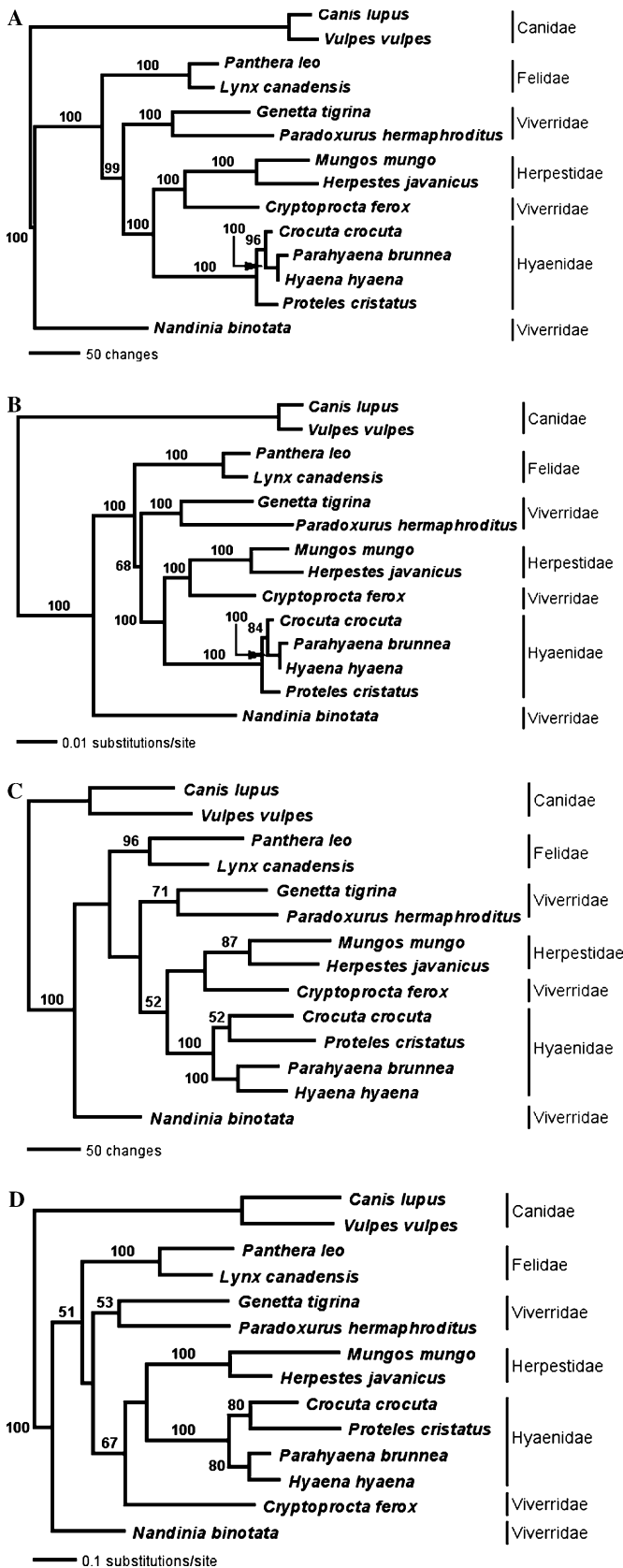


Fig. 1. (A) Maximum parsimony phylogram from analysis of concatenated nuclear gene data ($L = 1390$). (B) Maximum likelihood phylogram from analysis of concatenated nuclear gene data ($-\ln L = 14115.730$). (C) Maximum parsimony phylogram from analysis of the complete cytochrome *b* gene ($L = 1479$). (D) Maximum likelihood phylogram from analysis of the complete cytochrome *b* gene ($-\ln L = 7205.903$). Branch lengths are drawn proportional to the number of changes (parsimony, A and C) or the number of substitutions per site (likelihood, B and D); (see scale bars). Family affiliation of major clades and lineages are shown at the right of the tree. Bootstrap support values out of 1000 (A and C) or 300 (B and D) pseudoreplicates are shown above internodes.

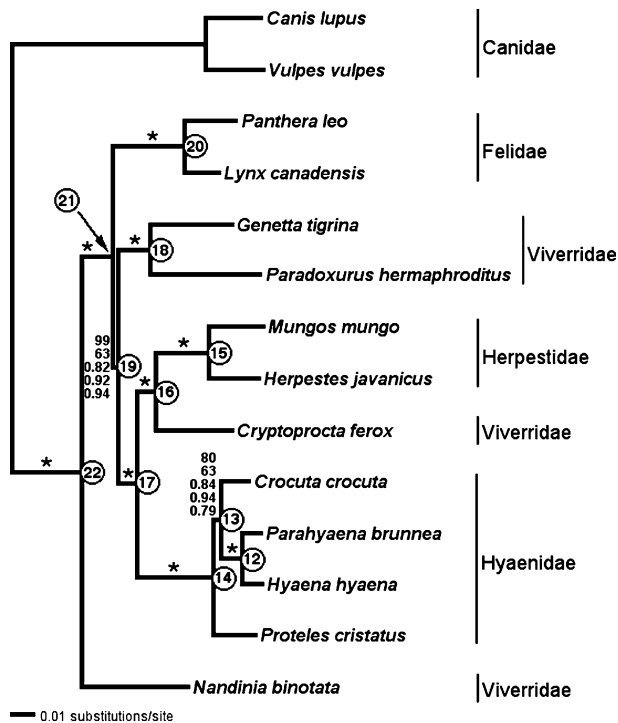


Fig. 2. Maximum likelihood phylogram inferred from analysis of the molecular supermatrix ($-\ln L = 22121.985$). Internodes with asterisks (*) indicate maximal bootstrap support (100%) from parsimony and likelihood analyses (1000 and 300 pseudoreplicates, respectively) and 1.00 posterior probability values from Bayesian analyses using Model 1, Model 2, and Model 3 (see Section 2). Uncircled numbers shown at nodes 13 and 19 are, from top to bottom, maximum parsimony bootstrap, maximum likelihood bootstrap, and node posterior probability values using Models 1, 2, and 3, respectively. Circled numbers 12–22 indicate dated nodes referred to in Table 6. Branch lengths are drawn proportional to the number of substitutions per site (see scale bar). Family affiliation of major clades and lineages are shown at the right of the tree.

In all phylogenetic analyses of the supermatrix, *Nandinia* was the most basal taxon within the feliforms, followed by a clade containing the two felids, which formed the sister group to the viverrids (*Genetta* and *Paradoxurus*), herpestids and hyaenids. The two herpestids and *Cryptoprocta* were the sister group to the hyaenids. Based on the distribution of the four viverrid taxa that we included in our analyses, our results clearly suggest that the Viverridae, as defined in current classifications (e.g., Corbert and Hill, 1991; Wozencraft, 1993), is paraphyletic. Within hyaenids, *Proteles* was basal and sister to a clade in which *Crocuta* formed the sister group to *Parahyaena* plus *Hyaena* (Fig. 2).

All but two of the nodes in the supermatrix tree were supported by 100% MP and ML bootstrap values or 1.00 posterior probabilities in the Bayesian analyses (Fig. 2). The two nodes that received less than maximal support were the same ones as those in the trees based on the concatenated nuclear data (see Figs. 1A and B), specifically the node between the felid clade and the clade of the remaining feliforms except *Nandinia* (node 19) and the node between *Proteles* and the remaining hyaenids (node 13). Bootstrap

Table 4

Unambiguous synapomorphies for two clades within the Hyaenidae

(Crocuta crocuta (Hyaena hyaena, Parahyaena brunnea))

APOB: 745, C → A

GHR: 1757, C → T; 1759, 1 → 0; 2232, G → A

GNAT1: 2581, C → T

CYT *b*: 4728, A → G; 5113, C → T; 5166, A → G; 5577, A → G; 5619, A → G*(Hyaena hyaena, Parahyaena brunnea)*

APOB: 605, A → G

CHRNA1: 1096, T → C; 1212, A → C

COL10A1: 1571, G → A

RAG1: 2724, A → G; 2872, C → T

CYT *b*: 5025, C → T; 5310, A → G; 5415, A → G; 5470, C → T; 5497, A → G; 5559, C → T

The locus, the number corresponding to the base pair position in the gap-coded alignment of the supermatrix, and the nucleotide transition are listed below the Newick representation of the clade.

values and posterior probability for these nodes varied among the methods used to analyze the supermatrix. Nodes 19 and 13 received strong bootstrap support in the MP analyses (99 and 80%, respectively), but relatively low support in the ML analyses (63% each). We used the “list of apomorphies” output in PAUP* from the MP analyses to examine the nature of nucleotide changes along the two internal nodes *within* the Hyaenidae (i.e., nodes 13 and 12 in Fig. 2). These nodes were supported by 10 and 12 unambiguous synapomorphies, respectively (Table 4). Of the 22 unambiguous synapomorphies, half of these were from the *cyt b* gene, while the remainders were contributed by various nuclear gene segments. The majority of changes were transitions ($A \leftrightarrow G$ or $C \leftrightarrow T$), two were transversions ($A \leftrightarrow C$) and a single indel in the GHR locus contributed support to the clade that placed *Crocuta* as the sister to *Hyaena* plus *Parahyaena*.

Burn-in plots (not shown) from MCMC chains using models 1 and 2 showed that chain likelihood scores reached stationarity within 100,000 generations and usually by 50,000 or 60,000 generations. For model 3, however, chain likelihood scores did not achieve stationarity until about 250,000 generations. This result suggests that longer mixing of MCMC chains was required for Model 3, most likely due to the increased number of parameters that had to be estimated. Therefore, consensus topologies, likelihood scores and parameter estimates from the three independent MCMC runs conducted for each model are based on 9000 post burn-in trees (after discarding the first 1000 trees) for Models 1 and 2, but only 7000 post burn-in trees for Model 3 (after discarding the first 3000 trees). There was a clear improvement in the chain likelihood scores from Model 1 (GTR + I + G) to Model 3 (GTR + partition-codonSSG) in which the among-site rate variation was partitioned among the nuclear gene segments plus the three codon positions of *cyt b* (Table 5). The post burn-in estimates of the likelihood and nucleotide substitution model parameter values were generally consistent among the three independent MCMC runs for GTR + I + G and GTR + partition SSG models, but these varied more for the GTR + partition-codonSSG

Table 5

Parameter estimates (mean and 95% credibility intervals) for each of three MCMC runs using the three substitution models: GTR + I + G; GTR with among site rate variation partitioned among the eight gene segment partitions (GTR + partitionSSG); and GTR with among site rate variation partitioned among the seven nuclear gene segments and the three codon positions of the *cyt b* gene (GTR + partition-codonSSG)

	Run 1	Run 2	Run 3
<i>GTR + I + G</i>			
–ln Likelihood	–22141.149 (–22151.010 to –22133.310)	–22141.052 (–22150.880 to –22133.060)	–22141.031 (–22151.000 to –22133.560)
π_A	0.271 (0.261–0.282)	0.272 (0.261–0.282)	0.272 (0.262–0.282)
π_C	0.245 (0.235–0.255)	0.245 (0.235–0.255)	0.245 (0.236–0.255)
π_G	0.221 (0.211–0.231)	0.221 (0.211–0.231)	0.221 (0.212–0.231)
π_T	0.262 (0.251–0.273)	0.262 (0.252–0.273)	0.262 (0.252–0.273)
I	0.443 (0.372–0.505)	0.444 (0.375–0.507)	0.444 (0.373–0.505)
G	0.647 (0.492–0.843)	0.650 (0.498–0.853)	0.648 (0.494–0.844)
Γ_{AC}	2.850 (2.160–3.803)	2.801 (2.127–3.625)	2.814 (2.133–3.618)
Γ_{AG}	6.624 (5.150–8.584)	6.520 (5.099–8.278)	6.554 (5.092–8.168)
Γ_{AT}	0.955 (0.675–1.320)	0.936 (0.662–1.294)	0.946 (0.674–1.261)
Γ_{CG}	0.749 (0.481–1.093)	0.736 (0.500–1.072)	0.751 (0.493–1.055)
Γ_{CT}	12.308 (9.696–16.015)	12.088 (9.469–15.207)	12.202 (9.519–15.202)
Γ_{GT}	1	1	1
<i>GTR + partitionSSG</i>			
–ln Likelihood	–21740.559 (–21764.820 to –21725.700)	–21734.731 (–21750.000 to –21725.450)	–21736.046 (–21748.370 to –21727.340)
π_A	0.279 (0.268–0.290)	0.281 (0.270–0.293)	0.280 (0.269–0.290)
π_C	0.260 (0.250–0.270)	0.264 (0.253–0.274)	0.261 (0.251–0.271)
π_G	0.208 (0.198–0.218)	0.204 (0.195–0.214)	0.207 (0.198–0.217)
π_T	0.253 (0.243–0.262)	0.251 (0.242–0.261)	0.253 (0.242–0.263)
G	0.323 (0.286–0.364)	0.326 (0.291–0.363)	0.326 (0.289–0.367)
Γ_{AC}	1.890 (1.503–2.355)	1.609 (1.269–2.034)	1.794 (1.355–2.305)
Γ_{AG}	6.303 (5.060–7.837)	6.009 (4.863–7.424)	6.148 (4.796–7.725)
Γ_{AT}	0.792 (0.571–1.073)	0.714 (0.499–0.973)	0.760 (0.553–1.019)
Γ_{CG}	0.672 (0.473–0.953)	0.618 (0.436–0.864)	0.655 (0.453–0.891)
Γ_{CT}	9.436 (7.482–11.592)	8.645 (6.952–10.777)	9.131 (7.153–11.325)
Γ_{GT}	1	1	1
SS1 (APOB)	0.510 (0.350–0.750)	0.390 (0.338–0.551)	0.438 (0.410–0.499)
SS2 (CHRNA1)	0.962 (0.846–1.261)	0.892 (0.806–1.175)	1.069 (0.900–1.155)
SS3 (COL10A1)	0.565 (0.329–0.780)	0.594 (0.290–0.900)	0.697 (0.545–0.908)
SS4 (GHR)	0.637 (0.433–0.719)	0.538 (0.519–0.737)	0.549 (0.481–0.671)
SS5 (GNAT1)	0.413 (0.348–0.485)	0.430 (0.310–0.509)	0.443 (0.309–0.503)
SS6 (RAG1)	0.442 (0.276–0.571)	0.354 (0.263–0.465)	0.414 (0.335–0.597)
SS7 (WT1)	0.664 (0.467–0.856)	0.573 (0.544–0.707)	0.678 (0.569–0.720)
SS8 (Cyt <i>b</i>)	2.855 (2.733–3.069)	3.196 (2.950–3.306)	2.933 (2.752–3.123)
<i>GTR + partition-codonSSG</i>			
–ln Likelihood	–21593.161 (–21605.710 to –21585.130)	–21604.171 (–21613.650 to –21596.130)	–21635.771 (–21684.410 to –21602.510)
π_A	0.284 (0.273–0.295)	0.281 (0.271–0.290)	0.280 (0.269–0.291)
π_C	0.263 (0.254–0.274)	0.263 (0.252–0.273)	0.260 (0.251–0.271)
π_G	0.203 (0.194–0.212)	0.207 (0.197–0.216)	0.208 (0.198–0.217)
π_T	0.249 (0.240–0.259)	0.249 (0.239–0.260)	0.252 (0.242–0.261)
G	0.553 (0.478–0.653)	0.485 (0.423–0.555)	0.479 (0.360–0.612)
Γ_{AC}	1.500 (1.138–1.987)	1.713 (1.295–2.295)	1.837 (1.436–2.262)
Γ_{AG}	5.611 (4.446–6.996)	6.007 (4.823–7.594)	6.199 (5.039–7.700)
Γ_{AT}	0.691 (0.497–0.928)	0.784 (0.569–1.095)	0.803 (0.585–1.066)
Γ_{CG}	0.624 (0.422–0.866)	0.659 (0.459–0.893)	0.696 (0.489–0.959)
Γ_{CT}	8.714 (6.847–10.868)	9.371 (7.493–11.860)	9.574 (7.595–11.963)
Γ_{GT}	1	1	1
SS1 (APOB)	0.630 (0.628–0.630)	0.491 (0.477–0.570)	0.461 (0.323–0.672)
SS2 (CHRNA1)	0.645 (0.549–1.725)	0.628 (0.462–1.364)	2.419 (0.770–4.254)
SS3 (COL10A1)	1.783 (0.748–1.870)	0.854 (0.622–0.872)	0.731 (0.254–1.072)
SS4 (GHR)	0.596 (0.586–0.734)	0.728 (0.708–0.810)	0.651 (0.443–0.986)
SS5 (GNAT1)	0.194 (0.163–0.194)	0.301 (0.202–0.480)	0.473 (0.358–0.683)
SS6 (RAG1)	0.415 (0.412–0.470)	0.532 (0.402–0.627)	0.442 (0.300–0.751)
SS7 (WT1)	0.577 (0.557–0.800)	0.704 (0.654–0.919)	0.694 (0.419–0.958)
SS8 (Cyt <i>b</i> codon 1)	1.783 (1.169–1.803)	3.487 (2.073–3.776)	1.949 (1.525–6.802)
SS9 (Cyt <i>b</i> codon 2)	0.379 (0.355–0.751)	0.419 (0.360–0.727)	0.823 (0.364–1.019)
SS10 (Cyt <i>b</i> codon 3)	6.021 (5.142–6.118)	4.341 (3.741–4.452)	4.162 (3.207–5.082)

Parameter abbreviations are the same as in Table 3, except SS1, SS2, ... = site specific gamma shape parameter.

model (Table 5). The same topology (Fig. 2) was recovered among the independent MCMC runs for each model as well as among the three models. The posterior probability values shown in Fig. 2 represent the final consensus values derived from the combination of results from the three separate runs for each model ($3 \times 9000 = 27,000$ trees for Models 1 and 2 and $3 \times 7000 = 21,000$ trees for Model 3). All but two nodes received 1.00 posterior probability support. The two nodes that had <1.00 posterior probability support differed greatly in their posterior probabilities according to the model implemented. For node 19, the posterior probability increased from 0.82 (Model 1) to 0.94 (Model 3). The posterior probability of node 13 increased from 0.84 with Model 1 to 0.94 with Model 2 but then decreased to 0.79 with Model 3 (Fig. 2). This suggests that, at least for these two nodes, the estimated posterior probability was sensitive to the way in which among-site rate variation was partitioned among or within the individual gene segments. However, as we noted above with regard to the phylogenetic results based on the concatenated nuclear data, these two nodes were estimated as the shortest branches on the tree (Fig. 2).

3.4. Analyses combining the molecular supermatrix and morphologic characters

When we combined the molecular supermatrix with the 29 morphological characters from the study by Werdelin and Solounias (1991), an exhaustive search using parsimony found the tree shown in Fig. 3. Relationships among the four hyaenids were identical to those based on the concatenated nuclear data and the supermatrix alone (Figs. 1A and B, and 2). Nodes defining hyaenid monophyly and grouping *Hyaena* plus *Parahyaena* received 100% parsimony bootstrap support, whereas the node between *Pro-*

teles and other hyaenids had a bootstrap support of 99%. Bremer support was similarly high for these nodes, but the PBS analyses revealed that the nine individual data sets differed in their relative contributions to total Bremer support at the nodes (Fig. 3). Each of the molecular data sets provided a large contribution to hyaenid monophyly, but among the 29 morphological characters, only 2 of these provided support for the monophyly of hyenas. The node between *Proteles* and other hyaenids had a Bremer support value of 14, and this node received the most support from the morphological data among the nine data partitions in the PBS analyses. Further, among the molecular data sets, CHRNA1 and COL10A1 provided conflicting information for this relationship based on their negative values whereas RAG1 and WT1 apparently contributed zero support. The loci that did contribute positive support to this node are the same ones that provided unambiguous synapomorphies for this node in the parsimony analyses of the supermatrix (Table 4). For the node that joins *Hyaena* and *Parahyaena* together in a clade, all molecular data sets contributed positive support, with *cyt b* contributing the most support. Interestingly, the phylogenetic signal from the morphological data contributes conflicting signal to this node, as evidenced by the PBS value of -3 (Fig. 3). We note, however, that the Bremer support and PBS values should be treated with caution because the statistical meaning of these values are unclear (DeBry, 2001). Nonetheless, Bremer support and PBS analyses together provide a rough means of evaluating the relative contributions of different data sets to the total nodal support of a tree in a combined analysis.

3.5. Divergence times

The relaxed clock estimates of divergence dates provided a detailed estimate of the timing of diversification of the four

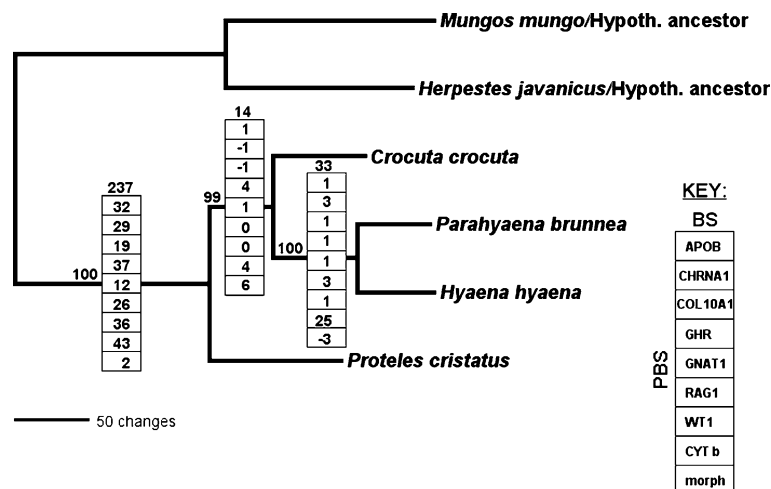


Fig. 3. Maximum parsimony phylogram inferred from analysis of the combined molecular supermatrix and modified morphological character matrix from Werdelin and Solounias (1991). For this tree, length (L)=918, consistency index (CI) excluding uninformative characters = 0.7960, and retention index (RI) = 0.7597. Numbers above internodes and to the left of boxes are bootstrap values (1000 pseudoreplicates). Numbers on top of boxes are Bremer support (BS) index values. Numbers inside boxes are partitioned Bremer support (PBS) values from the nine data partitions used in the combined analysis (see key). Branch lengths are drawn proportional to the number of changes (see scale bar). Morph = morphological data. Hypoth. ancestor = hypothetical ancestor.

Table 6

Summary of divergence dating results for hyaenids and related carnivorans obtained with a Bayesian relaxed clock approach using a molecular supermatrix and nine fossil calibrations (see Section 2)

Node/clade	Included taxa	Age (MYA)	CI (MYA)
12	<i>Hyaena</i> + <i>Parahyaena</i>	4.2	2.6–6.4
13	<i>Crocota</i> + <i>Hyaena</i> + <i>Parahyaena</i>	8.6	5.7–12.4
14	Hyaenidae	10.6	7.3–15.0
15	Core Herpestidae	11.8	8.1–16.7
16	<i>Cryptoprocta</i> + Core Herpestidae	24.4	18.3–32.2
17	Hyaenidae + Clade 16	29.2	22.5–37.9
18	Core Viverridae	25.2	18.9–33.2
19	Clades 17 + 18	35.2	27.7–45.1
20	Felidae	14.7	10.2–20.5
21	Felidae + Clade 19	36.5	28.9–46.5
22	<i>Nandinia</i> + Clade 21	43.3	33.4–54.1

Node numbers refer to clades indicated in Fig. 2. CI, credibility interval.

hyaena species, as well as their separation from the other feliform clades (Table 6, Fig. 2). Hyenas diverged from the core Herpestidae plus *Cryptoprocta* clade ca. 29.2 MYA, but the diversification of the four crown species is quite recent, at ca. 10.6 MYA (credibility interval [CI]: 7.3–15.0 MYA). This date corresponds to the node uniting *Proteles* to the remaining hyaenids, while the subsequent node (*Crocota* united to [*Hyaena* plus *Parahyaena*]) was estimated at 8.6 MYA (CI: 5.7–12.4 MYA), and the split between *Hyaena* and *Parahyaena* was estimated to have occurred ca. 4.2 MYA (CI: 2.6–6.4 MYA). Eleven different runs of the dating analysis produced consistent values, affirming the convergence of the Bayesian chains and congruence across varying combinations of fossil constraints. Importantly, in one of the alternative runs we released the upper limit (maximum) of 16.4 MYA for the base of crown Hyaenidae, to test whether our young dates for this clade could be biased due to use of this constraint. Results from this run were almost identical to the ones shown here, with point estimates and credible intervals for node ages differing by less than 1 million years from the values presented in Table 6. Modification of the mean of the prior distribution for ingroup root age from 50 to 25 MYA did produce detectable changes, however the effect was minor given the magnitude of the parameter change: point estimates for recent nodes (e.g., all those within the Hyaenidae) were shifted by 0.3–0.8 million years, whereas those for basal nodes in the Feliformia were moved by up to 4 million years.

4. Discussion

Phylogenetic analysis of the molecular supermatrix recovered the same topology of relationships among the four living hyaenids, regardless of the optimality criterion we used (Fig. 2). Among the three bone-cracking hyaenids, *Hyaena* and *Parahyaena* are joined together as sister taxa with maximum nodal support (100% MP and ML bootstrap and 1.00 Bayesian posterior probability), and *Crocota* is the more basal sister species to this clade. *Proteles* is the basal taxon in the extant Hyaenidae and is a very close sister species to the three bone-cracking species (Fig. 2). We find this same pat-

tern of relationships in the phylogenetic analysis with the concatenated nuclear gene data, also with high bootstrap support (Figs. 1A and B). The *cyt b* data support a slightly different topology, however, in which the basal node divides the hyaenids into two clades, one containing *Hyaena* plus *Parahyaena* and the other containing *Crocota* plus *Proteles*. This same topology was recovered in a previous phylogenetic study of hyaenids, also using the *cyt b* gene (Jenks and Werdelin, 1998). These authors attributed the pairing of *Crocota* with *Proteles* to a long-branch attraction artifact, possibly caused by the use of distant outgroups, *Felis catus*, a feliform carnivoran and *Phoca vitulina*, a caniform carnivoran, in their analyses. However, a topology that places *Proteles* in its generally accepted position at the base of the clade (as in our Fig. 2) was obtained when all transition substitutions were excluded or only third position transversions were analyzed (Jenks and Werdelin, 1998).

Our results challenge two widely accepted ideas concerning hyaenid relationships: first, that *Proteles* is a distantly related relict of an extinct clade of hyaenids, and second, that the highly autapomorphic *Crocota* is the most derived hyaenid. In addition, our analysis rejects the recent placement of *Hyaena* and *Crocota* as sister taxa (Werdelin and Solounias, 1991), and favors previous analyses that united *Hyaena* and *Parahyaena* as sister taxa (Ewer, 1955; Gaudry, 1862–1867; Hende, 1974; Pilgrim, 1932; Thenius, 1966). Below we discuss each of these findings, as well as our analysis of the interrelationships among feliform carnivorans, and the dating of these divergences.

4.1. The Position of *Proteles*

The fossil record and our data indicate that *Crocota*, *Hyaena*, *Parahyaena*, and *Proteles* are the living remnants of a diverse clade of medium to large sized highly carnivorous hyenas that were widespread in the Old World between 12 and 5 MYA (Werdelin and Solounias, 1991). The oldest known definitive fossil hyaenids in Africa are from the Middle Miocene (ca. 14 MYA), about five million years after tectonic activity established a land bridge (the Gomphothere Bridge) that connected Eurasia and Africa, facilitating faunal dispersal between the two continents for the first time (Agustí and Antón, 2002; Hunt, 1996; Turner and Antón, 2004). Based on the credibility interval for node 14 (Table 6), the four extant species appear to have originated in Africa 7–15 MYA, before the Early Pliocene (ca. 5 MYA), a time when hyaenids were diverse in Africa (Hunt, 1996).

Our results suggest that the aardwolf diverged much more recently (ca. 10.6 MYA) from its bone-cracking relatives than the inferred divergence time of ~18–20 MYA based on morphology (Werdelin and Solounias, 1991) or a molecular clock using third position transversions of the *cyt b* gene (Jenks and Werdelin, 1998). This has two important consequences for understanding the evolution of the aardwolf, which first appears in the African Pleistocene fossil record, ca. 1.5 MYA (Richardson, 1987a,b; Werdelin and Solounias, 1991). First, the younger age reduces the gap

between the estimated time of origin of the aardwolf and its earliest appearance in the fossil record to approximately nine million years, as opposed to 16.5–18.5 million years as implied by previous morphological studies (Werdelin and Solounias, 1991). Second, this result suggests that the aardwolf is derived from a more recently evolved group of hyaenids and thus challenges ideas about the morphological transition that led to the evolution of the aardwolf's unique ecology and associated craniodental morphology. Based on their morphological analyses of fossil and extant hyaenids, Werdelin and Solounias (1991) placed *Proteles* near the base of the hyaenid tree, in an unresolved position between *Plioviverrops* and other primitive hyaenids (e.g., *Tungurictis*, *Tongxinictis*, and *Thalassictis*). This position was favored because *Plioviverrops* species tended to be small insectivores and omnivores, and thus a transition to myrmecophagy seemed relatively plausible (Thenius, 1966; Werdelin and Solounias, 1991). In this view, the morphological adaptations associated with myrmecophagy are ancestral features retained from Middle to Late Miocene hyaenids (Werdelin and Solounias, 1991).

In contrast, our estimated divergence time suggests that the aardwolf may instead have a shared ancestry with the *Lycyaena-Chasmaporthetes* lineage, which were cursorial meat and bone eating hyaenids that first arose in the late Middle Miocene, ca. 11.8 MYA (Werdelin and Solounias, 1991, 1996). Fossils of *Lycyaena* first appear in north African deposits at around this time and then become more dominant in the Late Miocene and Pliocene of Africa (Werdelin and Solounias, 1991). Derivation of aardwolves from *Lycyaena* ancestors was originally proposed by Ewer and Cooke (1964) and later reiterated by Ewer (1973). In support of this relationship, aardwolves share the more derived dental formula with the three extant bone-cracking hyenas (Gingerich, 1974), which is characterized by fewer molars and premolars. However, Werdelin and Solounias (1991) considered the ancestry of *Proteles* from *Lycyaena* to be implausible because of the divergent craniodental morphology of *Lycyaena* compared to *Proteles*. If *Proteles* was a descendant of a taxon similar to *Plioviverrops* that had 6–7, rather than 4–5 cheek teeth as in the extant bone-cracking hyenas, more cheek teeth would be expected to be retained by *Proteles*, despite their reduction to pegs. In addition, the short branch length between the split of *Proteles* and *Crocota* suggests that *Proteles* shares a close common ancestry (ca. 2 million years) with the more derived bone-cracking hyaenids (Table 6).

Although our data suggest that *Proteles* may have had a more recent ancestry than previously thought, it does not indicate when *Proteles* acquired its unique dietary specialization. We suggest that the remarkable transition from meat eating carnivore to termite specialist may have occurred at a time when grassland ecosystems were becoming more widespread worldwide, including the sub-Saharan African savannas, from the Late Miocene to the Early Pleistocene (Jacobs et al., 1999; Potts and Behrensmeyer, 1992). Notably, >90% of the diet of aardwolves consists of

nasute harvester termites of the genus *Trinervitermes*, which consume grasses (Kruuk and Sands, 1972; Richardson, 1987a). These termites forage on the soil surface in dense concentrations, and consequently the aardwolf may ingest as many as 300,000 termites in a single night (Richardson, 1987b). *Trinervitermes* is thought to have evolved during the Late Miocene (Weesner, 1960) and is one of the most derived genera within the isopteran family Termitidae (B. Thorne, pers. Comm.). Therefore, the aardwolf may have evolved from carnivorous and/or bone-eating ancestors into a niche that was largely unexploited by other carnivores, possibly as a result of increased competition with other large carnivores, which reached their greatest diversity during the Pliocene (Hunt, 1996; Turner and Antón, 2004; Werdelin, 2003). A test of the hypothesis of coevolution between the aardwolf and *Trinervitermes* might be provided by reconstructing the phylogenetic history of the Termitidae as well as using this phylogeny to understand the evolution of foraging mode in this family of termites.

4.2. The evolution of *Crocota*

The spotted hyena appears to be the most derived of the living species based on unique features of its morphology and behavior (Werdelin and Solounias, 1991). Relative to the other two extant, bone-cracking species, *Crocota* is more specialized as a hypercarnivore, hunting for prey rather than scavenging, foraging in groups rather than alone, and regularly capturing prey larger than itself. This is reflected in its robust skull and teeth that easily crack very large bones and rapidly slice through tough skin (Werdelin, 1996a,b; Van Valkenburgh et al., 2004). Relative to striped and brown hyenas, spotted hyenas have a broader muzzle, larger carnassials, and enhanced jaw muscle mechanics (Van Valkenburgh et al., 2004). Beyond these feeding adaptations, spotted hyenas are unique in their extreme sexual monomorphism, in which females have masculinized genitalia associated with high levels of aggression. This collection of autapomorphies has led to the assumption that *Crocota* is the most specialized of the three bone-cracking hyaenids (Werdelin and Solounias, 1991). However, our phylogenetic analysis indicates otherwise; the divergence between *Crocota* and *Hyaena* plus *Parahyaena* occurred ca. 8.6 MYA (Table 6). Based on the fossil record, their common ancestor was likely an African bone-cracking species that split to form two lineages, one leading to the dominantly hunting *Crocota*, and the other to the dominantly scavenging *Hyaena* plus *Parahyaena* clade.

This evolutionary scenario presents some intriguing questions concerning the evolution of the unique genital monomorphism of *Crocota*. It has been argued that female masculinization evolved as a byproduct of selection for aggression when feeding at carcasses (Frank, 1986). Female spotted hyenas produce relatively large young that must be nourished with copious quantities of maternal milk. High levels of competitive aggression occurs during

group carcass feeding, and dominant females gain greater access to carcasses and raise more young successfully (Frank et al., 1995; Holekamp et al., 1996; Holekamp and Smale, 2000). Because there is no known osteological indicator of hyena masculinization at present, the origin of this trait cannot be determined. Moreover, there is evidence that both androgenic and nonandrogenic mechanisms are involved in the development of the penile clitoris of female *Crocota* (Drea et al., 1998, 1999). However, Frank's scenario would suggest that masculinization should have evolved concomitantly with the ability to cooperatively hunt large prey. It is also possible that the evolution of cooperative hunting and consequent feeding competition may have accelerated the evolution of an emerging suite of variations in the genitalia of female *Crocota* due to nonandrogenic mechanisms. The craniodental morphology of the earliest *Crocota* from the Late Pliocene of Africa and Asia (McKenna and Bell, 1997) is consistent with a group hunter of large prey and thus the genital monomorphism may have evolved very near to the origin of this species. It is also possible that genital monomorphism was present in the common ancestor of all three bone-crackers, but this would require a loss of multiple characters within the scavenging lineage. Surprisingly, no fossil or living intermediates have been found between either *Crocota* and other hyaenids or between *Proteles* and other hyaenids. The absence of intermediate forms for these unusual species suggests that the transitions were rapid (but see Werdelin and Solounias, 1991, who found morphological evolution within hyaenids to be generally gradual in nature). Indeed, given the short internal branch lengths and long terminal branch lengths for the Hyaenidae in our tree (Fig. 2), *Proteles* and *Crocota* may have acquired their autapomorphic morphologies well after their divergence. As noted above in the discussion of *Proteles*, the guild of large African carnivores was very diverse in the Pliocene. Intense competition for food could have driven the evolution of both the aardwolf and spotted hyena, with the former exiting the guild and the other evolving unique behaviors and morphology to succeed.

4.3. *Hyaena* and *Parahyaena* as sister taxa

With regard to relationships among *Crocota*, *Hyaena* and *Parahyaena*, our phylogeny contradicts the hypothesis of relationships based on cladistic analyses of morphological characters that either place *Hyaena* or *Parahyaena* as the sister taxon to *Crocota* (Galiano and Frailey, 1977; Werdelin and Solounias, 1991). In Werdelin and Solounias (1991) cladistic analysis of the four extant genera, trees in which either *Hyaena* or *Parahyaena* was paired with *Crocota* were equally parsimonious. However, these authors suggested that the tree in which *Hyaena* was paired with *Crocota* was better supported because these taxa shared three synapomorphies, relative to the two synapomorphies joining *Parahyaena* and *Crocota* together. In either case, these relationships were weakly supported. Nonetheless,

our tree is congruent with earlier views based on overall morphological similarity that suggested that *Parahyaena* and *Hyaena* are more closely related than either of these are to *Crocota* (Ewer, 1955; Gaudry, 1862–1867; Hendey, 1974; Pilgrim, 1932; Thenius, 1966).

Given the small number of extant taxa involved and research effort spanning more than 100 years, why have morphological studies of hyaenid phylogeny not been able to reach a consensus? Part of the answer lies with changing philosophies associated with methods of phylogeny reconstruction and how morphological character similarity among taxa are thus evaluated (e.g., phenetic similarity vs. shared ancestral and shared derived traits). Moreover, a thorough survey of craniodental and postcranial skeletal morphology revealed few phylogenetically informative characters available for inferring relationships among extant taxa (Werdelin and Solounias, 1991). The short time intervals between branching events among hyaenids as evidenced in our phylogeny and dating analyses suggests that there was little time for informative morphological characters to become fixed. Even though mitochondrial and nuclear sequence data unambiguously support *Hyaena* and *Parahyaena* as sister taxa, the PBS analysis of the combined molecular and morphological character matrices showed that the morphological data contributes conflicting signal to this relationship (Fig. 3).

Our phylogeny suggests that some morphological characters that have been traditionally used in hyaenid systematics should be reevaluated. The craniodental skeleton has been the primary focus of almost all morphologically based inferences of hyaenid phylogeny. This is because craniodental remains comprise the vast majority of evidence when it comes to fossil hyaenids and therefore aspects of the craniodental skeleton allow extinct and extant taxa to be analyzed simultaneously. The availability of a rich fossil record for the Hyaenidae as a whole has been critical to defining character states and accurately establishing polarities, particularly with regard to the four extant taxa (Werdelin and Solounias, 1991). Nevertheless, our phylogeny clearly indicates that the morphological characters that join either *Hyaena* or *Parahyaena* with *Crocota* in the analyses using only extant taxa are either homoplasies or shared ancestral character states (symplesiomorphies). For example, *Hyaena* and *Crocota* are united by the following character states: (1) anterior position of infraorbital foramina relative to the middle of the upper third premolar; (2) presence of a premaxillary-frontal suture; (3) large processes for the nuchal ligament; and (4) a straight scapular spine (Werdelin and Solounias, 1991; present study). Beyond the implication that the polarities of these characters should be reinterpreted, there is the more important question of whether these (and perhaps other) characters actually constitute homologies or homoiologies (Reidl, 1978). Homoiologies are non-heritable morphological similarities that result from similar epigenetic responses to environmental stimuli (Lieberman, 2000). Because bone has the ability to remodel in response to changes in mechanical loading, many

osseous features of the cranial and postcranial skeleton are potentially homologies (Gibbs et al., 2000; Lieberman, 2000). With regard to hyenas, for example, the size of the nuchal processes (coded as either small or large) that serve for the attachment of the neck musculature may reflect how these processes are mechanically loaded in different species of hyenas and which may itself be related to the behavioral function of these muscles. Similarities in nuchal processes (as well as scapular spine shape) between different species of hyena may be due to similar loading regimes rather than common ancestry (i.e., homology). Further, because of integrated development among individual skull bones, change in shape or structure of one bone is usually influenced by changes in neighboring bones (Lieberman, 2000). As a consequence, osseous characters that have been used in appraisals of hyaenid phylogeny, such as relative position of the infraorbital foramen in the maxilla bone and the presence or absence of a premaxillary-frontal suture, cannot be considered independent in the phylogenetic sense. This also makes it difficult to understand whether such characters represent true homologies.

Comparative studies of craniofacial development and the effects of mechanical loading in different species of hyena offer a potential approach to evaluate the homologous nature of skull characters and thus their usefulness in phylogenetic inference. Such integrated studies have proven especially useful in testing homologies in the cranial skeleton of hominids (Lieberman, 2000 and references therein). The study by Binder and Van Valkenburgh (2000) examining correlated changes in skull morphology and bite strength in captive juvenile and adult spotted hyenas is especially pertinent in this regard. If the ontogenetic approach employed by these researchers could be extended to brown and striped hyenas and perhaps be integrated with landmark analyses (e.g., O'Higgins, 2000), this would perhaps better illuminate the phylogenetic signal in the cranial skeleton of hyenas.

As noted above, *cyt b* data support a topology which conflicts with that produced by the supermatrix, in that the basal node divides the hyaenids into two clades, one containing *Hyaena* plus *Parahyaena* and the other containing *Crocota* plus *Proteles*. Given that the topology based on the supermatrix is the phylogenetic hypothesis with the greatest support based on molecular data, then the present study and the one by Jenks and Werdelin (1998) indicate that the *cyt b* sequences by themselves contain misleading phylogenetic signal with regard to hyaenid relationships. This misleading signal may stem from a combination of homoplasy in transitions at first and third codon positions (Jenks and Werdelin, 1998) and/or nonstationary base composition (this study). While model-based methods like ML are usually expected to mitigate problems associated with homoplasy, we found that this was not the case here (Fig. 1D) and showed that nonstationary base composition was a more likely cause of the misleading signal (see Section 3). In the parsimony analysis of the supermatrix, we found that *cyt b* sequences contain unambiguous synapomorphies for

the two internal nodes within the hyaenid phylogeny (Table 5). Furthermore, PBS analyses of a data matrix in which we combined molecular and morphological characters showed that the *cyt b* data contributed substantial and positive signal to these same two nodes (Fig. 3). Therefore, the *cyt b* data are consistent with the topology derived from the nuclear gene data when the former data set is combined with the latter but is inconsistent (at least in ML and equally weighted MP analyses) when analyzed alone. These findings support the idea that combining data from multiple genomes (mitochondrial and nuclear in animals, along with the chloroplast genome in plants) can overcome the location-dependent idiosyncrasies that may be particular to certain genomes or linkage groups (Cummings et al., 1995). Additionally, our study reinforces the notion that a single gene or linkage group is unlikely to contain robust phylogenetic signal for all levels of a phylogeny and underscores the importance of sampling multiple loci (Cummings et al., 1995; Rokas et al., 2003).

4.4. Interrelationships among the feliform carnivorans

Our results show that the clade containing *Herpestes*, *Mungos* and *Cryptoprocta* is placed as the sister group to the Hyaenidae with 100% nodal support (Fig. 2). Furthermore, we estimate that these clades diverged around 29 MYA, in the Middle Oligocene (Table 6). This age is somewhat older than the 25 MYA age suggested by the hyaenid fossil record (Werdelin and Solounias, 1991), but this latter age falls within our estimated credibility interval (Table 6). The joining of hyaenids and herpestids as sister taxa supports earlier phylogenetic estimates based on analyses of the auditory bulla (Hunt, 1989). Our results are also congruent with previous molecular studies using mitochondrial gene sequences (*cyt b* and ND2) and nuclear gene sequences (intron 1 of the transthyretin gene and exon 1 of the interphotoreceptor retinoid-binding protein) that sampled only *Crocota* as the sole representative of the Hyaenidae (Flynn and Nedbal, 1998; Gaubert and Veron, 2003; Yoder et al., 2003; Yu et al., 2004). The two genera of mongooses represented in our study (*Herpestes* and *Mungos*) are classified in the Herpestidae while the Malagasy-endemic carnivoran *Cryptoprocta* is traditionally classified as a member of the Viverridae. Our findings, however, confirm the results of a recent study of Malagasy Carnivora that showed that carnivorans endemic to Madagascar (traditionally classified in both the Herpestidae and Viverridae) are descended from a single common ancestor and share ancestry with the Herpestidae (Yoder et al., 2003). Furthermore, among the four viverrid taxa we sequenced in our study, *Nandinia* was the most basal lineage within the feliforms (Fig. 2). Collectively, our results lend additional support to the conclusions of several recent studies that have shown that the Viverridae, as traditionally circumscribed, is not monophyletic (Flynn and Nedbal, 1998; Gaubert and Veron, 2003; Yoder et al., 2003; Yu et al., 2004). Overall, the pattern of interrelationships among the feliform families inferred in this study are concordant with these other molec-

ular-based studies, suggesting that different regions of the feliform carnivoran genome are tracking the same phylogenetic history. Although a larger sample of feliform taxa is obviously required to further validate these findings, such concordance across different studies nonetheless provides confidence that a stable phylogenetic hypothesis for the primary families of the Feliformia is emerging.

Acknowledgments

We are grateful to the individuals and institutions listed in Table 1 for providing the tissue and/or DNA samples used in this study. We thank P. Adam and C. Bardeleben for comments and editorial suggestions that improved the manuscript. This study was supported by research funds from the U.S. National Science Foundation.

Appendix A. Supplementary material

Supplementary data associated with this article can be found, in the online version, at [doi:10.1016/j.ympev.2005.10.017](https://doi.org/10.1016/j.ympev.2005.10.017).

References

- Agustí, J., Antón, M., 2002. Mammoths, Sabertooths, and Hominids: 65 Million Years of Mammalian Evolution in Europe. Columbia Univ. Press, New York, NY.
- Akaike, H., 1974. A new look at the statistical model identification. *IEEE Trans. Autom. Contr.* 19, 716–723.
- Amrine-Madsen, H., Koepfli, K.-P., Wayne, R.K., Springer, M.S., 2003. A new phylogenetic marker, apolipoprotein B, provides compelling evidence for eutherian relationships. *Mol. Phylogenet. Evol.* 28, 225–240.
- Barriel, V., 1994. Molecular phylogenies and how to code insertion/deletion events. *Life Sci.* 317, 693–701.
- Binder, W.J., Van Valkenburgh, B., 2000. Development of bite strength and feeding behaviour in juvenile spotted hyenas (*Crocuta crocuta*). *J. Zool. Lond.* 252, 273–283.
- Bininda-Emonds, O.R.P., Gittleman, J.L., Purvis, A., 1999. Building large trees by combining phylogenetic information: a complete phylogeny of the extant Carnivora (Mammalia). *Biol. Rev.* 74, 143–175.
- Bremer, K., 1988. The limits of amino acid sequence data in angiosperm phylogenetic reconstruction. *Evolution* 42, 795–803.
- Brouillette, J.A., Andrew, J.R., Venta, P.J., 2000. Estimate of nucleotide diversity in dogs with a pool-and-sequence method. *Mammal. Genome* 11, 1079–1086.
- Brown, J.H., Lomolino, M.V., 1998. Biogeography. Sinauer Associates, Sunderland, MA.
- Corbert, G.B., Hill, J.E., 1991. A World List of Mammalian Species. Oxford University Press, London.
- Cummings, M.P., Otto, S.P., Wakeley, J., 1995. Sampling properties of DNA sequence data in phylogenetic analysis. *Mol. Biol. Evol.* 12, 814–822.
- DeBry, R.W., 2001. Improving the interpretation of the decay index for DNA sequence data. *Syst. Biol.* 50, 742–752.
- DeBry, R.W., Olmstead, R.G., 2000. A simulation study of reduced tree-search effort in bootstrap resampling analysis. *Syst. Biol.* 49, 171–179.
- Drea, C.M., Weldele, M.L., Forger, N.G., Coscia, E.M., Frank, L.G., Glickman, S.E., 1998. Androgens and masculinization of genitalia in the spotted hyaena (*Crocuta crocuta*). 2. Effects of prenatal anti-androgens. *J. Reprod. Fert.* 113, 117–127.
- Drea, C.M., Corsica, E.M., Glickman, S.E., 1999. Hyenas. In: Knobil, E., Neill, J.D. (Eds.), *Encyclopedia of Reproduction* Vol. 2. Academic Press, San Diego, CA, pp. 718–725.
- Ewer, R.F., 1955. The fossil carnivores of the Transvaal caves. The lycyaenas of Sterkfontein and Swartkrans, together with some general considerations of the Transvaal fossil hyaenids. *Proc. Zool. Soc. Lond.* 124, 839–857.
- Ewer, R.F., 1973. The Carnivores. Cornell Univ. Press, Ithaca, NY.
- Ewer, R.F., Cooke, H.B.S., 1964. The Pleistocene mammals of southern Africa. In: Davis, D.H.S. (Ed.), *Ecological Studies in Southern Africa*. W. Junk, The Hague, pp. 35–48.
- Felsenstein, J., 1978. Cases in which parsimony and compatibility methods will be positively misleading. *Syst. Zool.* 27, 401–410.
- Flynn, J.J., Nedbal, M.A., 1998. Phylogeny of the Carnivora (Mammalia): congruence vs incompatibility among multiple data sets. *Mol. Phylogenet. Evol.* 9, 414–426.
- Frank, L.G., 1986. Social organization of the spotted hyaena (*Crocuta crocuta*) II. Dominance and reproduction. *Anim. Behav.* 35, 1510–1527.
- Frank, L.G., Holekamp, K.E., Smale, L., 1995. Dominance, demography and reproductive success of female spotted hyenas. In: Sinclair, A.R.E., Arcese, P. (Eds.), *Serengeti II: Dynamics, Management, and Conservation of an Ecosystem*. Univ. Chicago Press, Chicago, IL, pp. 364–384.
- Galiano, H., Frailey, D., 1977. *Chasmaporthetes kani*, new species from China, with remarks on the phylogenetic relationships of genera within the Hyaenidae (Mammalia, Carnivora). *Am. Mus. Nov.* 2632, 1–16.
- Gaubert, P., Veron, G., 2003. Exhaustive sample set among Viverridae reveals the sister-group of felids: the linsangs as a case of extreme morphological convergence within Feliformia. *Proc. R. Soc. Lond. B* 270, 2523–2530.
- Gaudry, A., 1862–1867. Animaux fossiles du Mont Leberon. F. Savy, Paris, France.
- Gingerich, P.D., 1974. *Proteles cristatus* Sparrman from the Plesitocene of South Africa, with a note on tooth replacement in the aardwolf (Mammalia: Hyaenidae). *Ann. Transvaal Mus.* 29, 49–55.
- Gibbs, S., Collard, M., Wood, B., 2000. Soft-tissue characters in higher primate phylogenetics. *Proc. Natl. Acad. Sci. USA* 97, 11130–11132.
- Hendey, Q.B., 1974. The late Cenozoic Carnivora of the southwestern Cape Province. *Ann. South Afr. Mus.* 63, 1–369.
- Holekamp, K.E., Smale, L., Szykman, M., 1996. Rank and reproduction in the female spotted hyaena. *J. Reprod. Fert.* 108, 229–237.
- Holekamp, K.F., Smale, L., 2000. Feisty females and meek males: reproductive strategies in the spotted hyena. In: Wallen, K., Schneider, K., Schneider, J. (Eds.), *Reproduction in Context*. The MIT Press, Cambridge, MA, pp. 257–285.
- Huelsenbeck, J.P., 2000. MrBayes: Bayesian inference of phylogeny. *Biometrics* 17, 754–755.
- Huelsenbeck, J.P., Ronquist, F., Nielsen, R., Bollbeck, J.P., 2001. Bayesian inference of phylogeny and its impact on evolutionary biology. *Science* 294, 2310–2314.
- Hunt Jr., R.M., 1987. Evolution of the Aeluroid Carnivora: significance of auditory structure in the nimravid cat *Dinictis*. *Am. Mus. Novitates* 2886, 1–74.
- Hunt Jr., R.M., 1989. Evolution of the Aeluroid Carnivora: Significance of the ventral promontorial process of the petrosal, and the origin of basicranial patterns in the living families. *Am. Mus. Novitates* 2930, 1–32.
- Hunt Jr., R.M., 1996. Biogeography of the Order Carnivora. In: Gittleman, J.L. (Ed.), *Carnivore Behavior, Ecology and Evolution*, vol. 2. Cornell Univ. Press, Ithaca, NY, pp. 485–541.
- Irwin, D.M., Kocher, T.D., Wilson, A.C., 1991. Evolution of the cytochrome *b* gene of mammals. *J. Mol. Evol.* 32, 128–144.
- Jacobs, B.F., Kingston, J.D., Jacobs, L.L., 1999. The origin of grass-dominated ecosystems. *Ann. Missouri Bot. Gard.* 86, 590–643.
- Jenks, S.M., Werdelin, L., 1998. Taxonomy and systematics of living hyaenas (Family Hyaenidae). In: Mills, M.G.L., Hofer, H. (Compilers), *Hyaenas: Status Survey and Conservation Action Plan*. IUCN/SSC Hyaena Specialist Group, IUCN, Gland, Switzerland, pp. 8–17.
- Jiang, Z., Priat, C., Galibert, F., 1998. Traced orthologous amplified sequence tags (TOASTs) and mammalian comparative maps. *Mammal. Genome* 9, 577–587.
- Kishino, H., Thorne, J.L., Bruno, W.J., 2001. Performance of a divergence time estimation method under a probabilistic model of rate evolution. *Mol. Biol. Evol.* 18, 352–361.

- Kluge, A.G., 1998. Total evidence or taxonomic congruence: cladistics or consensus classification. *Cladistics* 14, 151–158.
- Kocher, T.D., Thomas, W.K., Meyer, A., Edwards, S.V., Paabo, S., Villablanca, F.X., Wilson, A., 1989. Dynamics of mitochondrial DNA evolution in animals: amplification and sequencing with conserved primers. *Proc. Natl. Acad. Sci. USA* 86, 6196–6200.
- Koehler, C.E., Richardson, P.R.K., 1990. *Proteles cristatus*. *Mammal. Species* 363, 1–6.
- Koepfli, K.-P., Wayne, R.K., 1998. Phylogenetic relationships of otters (Carnivora: Mustelidae) based on mitochondrial cytochrome *b* sequences. *J. Zool.* 246, 401–416.
- Kruuk, H., 1972. The Spotted Hyena. Univ. of Chicago Press, Chicago, IL.
- Kruuk, H., Sands, W.A., 1972. The aardwolf (*Proteles cristatus* Sparrman) 1783 as a predator of termites. *E. Afr. Wildl. J.* 10, 211–227.
- Lake, J.A., 1994. Reconstructing evolutionary trees from DNA and protein sequences: paralinear Distances. *Proc. Natl. Acad. Sci. USA* 91, 1455–1459.
- Lieberman, D.E., 2000. Ontogeny, homology and phylogeny in the hominid craniofacial skeleton: the problem of the browridge. In: O'Higgins, P., Cohn, M.J. (Eds.), *Development, Growth and Evolution*. Academic Press, San Diego, CA, pp. 85–122.
- Lockhart, P.J., Steel, M.A., Hendy, M.D., Penny, D., 1994. Recovering evolutionary distances under a more realistic model of sequence evolution. *Mol. Biol. Evol.* 11, 605–612.
- Lyons, L.A., Laughlin, T.F., Copeland, N.G., Jenkins, N.A., Womack, J.E., O'Brien, S.J., 1997. Comparative anchor tagged sequences (CATS) for integrative mapping of mammalian genomes. *Nat. Genet.* 15, 47–56.
- McKenna, M.C., Bell, S.K., 1997. *Classification of Mammals Above the Species Level*. Columbia Univ. Press, New York, NY.
- Mills, M.G.L., 1982. *Hyaena brunnea*. *Mammalian Species* 194, 1–5.
- Mills, M.G.L., 1990. Kalahari Hyenas: comparative behavior and ecology of two species. Unwin-Hyden, London.
- Mills, M.G.L., 1999. The Brown Hyena. *Africa Environ. Wildl.* 7, 80–88.
- O'Higgins, P., 2000. Quantitative approaches to the study of craniofacial growth and evolution: advances in morphometric techniques. In: O'Higgins, P., Cohn, M.J. (Eds.), *Development, Growth and Evolution*. Academic Press, San Diego, CA, pp. 163–185.
- Pilgrim, G.E., 1932. The fossil Carnivora of India. *Paleont. Indica* 18, 1–232.
- Posada, D., Crandall, K.A., 1998. MODELTEST: testing the model of DNA substitution. *Bioinformatics* 14, 817–818.
- Potts, R., Behrensmeyer, A.K., 1992. Late cenozoic terrestrial ecosystems. In: Behrensmeyer, A.K., Damuth, J.D., DiMichele, W.A., Potts, R., Sues, H.-D., Wing, S.L. (Eds.), *Terrestrial Ecosystems Through Time: Evolutionary Paleocology of Terrestrial Plants and Animals*. Univ. of Chicago Press, Chicago, IL, pp. 419–541.
- Reidl, R.J., 1978. *Order in Living Organisms*. Wiley, New York, NY.
- Richardson, P.R.K., 1987a. Food consumption and seasonal variation in the diet of the aardwolf *Proteles cristatus* in southern Africa. *Z. Säugetierk.* 52, 307–325.
- Richardson, P.R.K., 1987b. Aardwolf: the most highly specialized myrmecophilous mammal? *South Afr. J. Sci.* 83, 405–410.
- Richardson, P.R.K., Coetsee, E.M., 1988. Mate desertion in response to female promiscuity in the socially monogamous aardwolf. *S. Afr. J. Zool.* 23, 306–308.
- Rieger, I., 1981. *Hyaena hyaena*. *Mammalian Species* 150, 1–5.
- Rokas, A., Williams, B.L., King, N., Carroll, S.B., 2003. Genome-scale approaches to resolving incongruence in molecular phylogenies. *Nature* 425, 798–804.
- Ronquist, F., Huelsenbeck, J.P., 2003. MrBayes 3: Bayesian phylogenetic inference under mixed models. *Bioinformatics* 19, 1572–1574.
- Rzhetsky, A., Nei, M., 1992. A simple method for estimating and testing minimum-evolution trees. *Mol. Biol. Evol.* 9, 945–967.
- Schlosser, M., 1890. Die Affen, Lemuren, Chiropteren, Insectivoren, Marsupialier, Creodonten und Carnivoren des europäischen Tertiärs. III. Beiträge zur Paläontologie und Geologie Österreich-Ungarns und des Orients 8, 1–107.
- Simpson, G.G., 1953. *The Major Features of Evolution*. Simon and Schuster, New York, NY.
- Sorenson, M.D. 1998. TreeRot, version 2. Univ. of Michigan, Ann Arbor, MI.
- Springer, M.S., Murphy, W.J., Eizirik, E., O'Brien, S.J., 2003. Placental mammal diversification and the Cretaceous-Tertiary boundary. *Proc. Natl. Acad. Sci. USA* 100, 1056–1061.
- Swofford, D.L., Olsen, G.J., Waddell, P.J., Hillis, D.M., 1996. Phylogenetic inference. In: Hillis, D.M., Moritz, C., Mable, B.K. (Eds.), *Molecular Systematics*. Sinauer Associates, Sunderland, MA, pp. 407–514.
- Swofford, D.L. 2002. PAUP*. *Phylogenetic Analysis Using Parsimony (* and Other Methods)*, Version 4.0. Sinauer Associates, Sunderland, MA.
- Teeling, E.C., Scally, M., Kao, D.J., Romagnoli, M.L., Springer, M.S., 2000. Molecular evidence regarding the origin of echolocation and flight in bats. *Nature* 403, 188–192.
- Thenius, E., 1966. Zur Stammesgeschichte der Hyänen (Carnivora, Mammalia). *Z. Säugetierk.* 31, 293–300.
- Thorne, J.L., Kishino, H., Painter, I.S., 1998. Estimating the rate of evolution of the rate of molecular evolution. *Mol. Biol. Evol.* 15, 1647–1657.
- Turner, A., 1987. New fossil carnivore remains from Plio-Pleistocene deposits in the Sterkfontein Valley (Mammalia: Carnivora). *Ann. Transvaal Mus.* 34, 203–226.
- Turner, A., Antón, M., 2004. *Evolving Eden: An Illustrated Guide to the Evolution of the African Large-Mammal Fauna*. Columbia Univ. Press, New York, NY.
- Van Valkenburgh, B., Wang, X., Damuth, J., 2004. Cope's rule, hypercarnivory, and extinction in North American canids. *Science* 306, 101–104.
- Venta, P.J., Brouillette, J.A., Yuzbasiyan-Gurkan, V., Brewer, G.J., 1996. Gene-specific universal mammalian sequence-tagged sites: application to the canine genome. *Biochem. Genet.* 34, 321–341.
- Wayne, R.K., Benveniste, R.E., Janczewski, D.N., O'Brien, S.J., 1989. Molecular and biochemical evolution of the Carnivora. In: Gittleman, J.L. (Ed.), *Carnivore Behavior, Ecology and Evolution*. Cornell Univ. Press, Ithaca, NY, pp. 465–494.
- Weesner, F.M., 1960. Evolution and biology of termites. *Ann. Rev. Entomol.* 5, 153–170.
- Werdelin, L., 1996a. Carnivoran ecomorphology: a phylogenetic perspective. In: Gittleman, J.L. (Ed.), *Carnivore Behavior, Ecology and Evolution*, vol. 2. Cornell Univ. Press, Ithaca, NY, pp. 582–624.
- Werdelin, L., 1996b. Community-wide character displacement in Miocene hyaenas. *Lethaia* 29, 97–106.
- Werdelin, L., Solounias, N., 1991. The Hyaenidae: Taxonomy, systematics and evolution. *Fossils and Strata* 30, 1–104.
- Werdelin, L., Solounias, N., 1996. The evolutionary history of hyaenas in Europe and western Asia during the early Miocene. In: Bernor, R.L., Fahlbusch, V., Mittmann, H.-W. (Eds.), *The Evolution of Western Eurasian Neogene Mammal Faunas*. Columbia Univ. Press, New York, NY, pp. 290–306.
- Werdelin, L., 2003. Mio-Pliocene Carnivora from Lothagam, Kenya. In: Leakey, M.G., Harris, J.M. (Eds.), *Lothagam: The Dawn of Humanity in Eastern Africa*. Columbia Univ. Press, New York, NY, pp. 261–678.
- Wozencraft, W.C., 1993. Carnivora. In: Wilson, D.E., Reeder, D.M. (Eds.), *Mammal Species of the World: A Taxonomic and Geographic Reference*. Smithsonian Institution Press, Washington, DC, pp. 279–348.
- Wurster, D.H., Benirschke, K., 1968. Comparative cytogenetic studies in the Order Carnivora. *Chromosoma* 24, 336–382.
- Wyss, A.R., Flynn, J.J., 1993. A phylogenetic analysis and definition of the Carnivora. In: Szalay, F.S., Novacek, M.J., McKenna, M.C. (Eds.), *Mammal Phylogeny: Placentalia*. Springer-Verlag, New York, NY, pp. 32–52.
- Yoder, A.D., Burns, M.M., Zehr, S., Delefosse, T., Veron, G., Goodman, S.M., Flynn, J.J., 2003. Single origin of Malagasy Carnivora from an African ancestor. *Nature* 421, 734–737.
- Yu, L., Li, Q.-w., Ryder, O.A., Zhang, Y.-p., 2004. Phylogenetic relationships within the mammalian order Carnivora indicated by sequences of two nuclear genes. *Mol. Phylogenet. Evol.* 33, 694–705.